Evaluation of ^{224}Ra as a tracer for submarine groundwater discharge in Long Island Sound (NY)

Garcia-Orellana J.[1,2,], Cochran J.K.[3], Daniel J.W.R.[3], Rodellas V.[1,2], Bokuniewicz H.[3], Heilbrun C.[3]*

[1] Departament de Física, Universitat Autònoma de Barcelona, E-08193 Bellaterra, Spain.

[2] Institut de Ciència i Tecnologia Ambientals (ICTA), Universitat Autònoma de Barcelona, E-08193 Bellaterra, Spain.

[3] School of Marine and Atmospheric Sciences, Stony Brook University, Stony Brook, New York, 11794-5000 USA.

*Corresponding author. Tel (+34) 935868285, Fax (+34) 935812155.
E-Mail address: jordi.garcia@uab.cat

ABSTRACT

The approach to quantify submarine groundwater discharge using Ra isotopes generally involves developing a Ra mass balance in an estuary, bay or lagoon. In this work we present a ^{224}Ra mass balance used to evaluate the importance of the submarine groundwater discharge (SGD) in Long Island Sound (NY, US), the third most important estuary in US, located between Long Island and Connecticut, and affected by summertime hypoxia in the western basin. Three surveys were conducted between April 2009 and August 2010 where 25 water stations were sampled for Ra isotopes, oxygen and Mn. Stations were oriented along 4 transects: one axial extending from the western to eastern Sound and three longitudinal transects in the western, central and eastern Sound.

The inventory of ^{224}Ra in the water column in summer was circa 2 times greater than in winter, suggesting an increased ^{224}Ra flux to the Sound in summer. A mass balance for ^{224}Ra was constructed considering tidal exchange, inputs from rivers, desorption from resuspended particles, diffusive fluxes (including bioirrigation) from bottom sediments and radioactive decay in the water column. Fluxes of ^{224}Ra from bottom sediments were measured by incubating cores under oxic conditions in a continuous flow mode such that the overlying water was circulated through a Mn-oxide fiber to maintain a constant activity of ^{224}Ra. Fluxes from muddy sediments (comprising ~67% of the Sound bottom) ranged from 127 to 312 dpm m^{-2} d^{-1} and were ~60 dpm m^{-2}·d^{-1} in sandy sediments (33% of the Sound). Incubations under hypoxic conditions showed variable fluxes depending on reduction and mobilization of Mn. The ^{224}Ra mass balance shows a net input of Ra to the Sound of 106 ± 50 ·10^{12} dpm y^{-1} in spring and 244 ± 112 ·10^{12} dpm y^{-1} in the summer that is attributed to SGD. Elevated ^{224}Ra values were observed near shore and in the pore fluids of the coarse beach sands along the Long Island and Connecticut coasts, suggesting that SGD driven by

tidal recirculation through the beach face is a major source of ^{224}Ra to the Sound. Seasonal variation in this source seems unlikely, and the calculated ^{224}Ra SGD fluxes for spring and summer overlap within the uncertainties. Nevertheless we conclude that variations in the ^{224}Ra water column inventories could be produced by seasonal changes in bioirrigation due to the increase of the benthonic productivity in summer and/or redox cycling of Mn as well as sediment resuspension and desorption of ^{224}Ra from resuspended particles, and that our mass balance underestimates these terms, particularly in the summer. ^{224}Ra fluxes from sediments in estuaries, especially those with significant areas of muddy sediments and seasonal hypoxia, are important and should be well constrained in future uses of this isotope as a tracer for SGD.

1. INTRODUCTION

The phenomenon of submarine groundwater discharge (SGD) has been shown to be an important component of the hydrological cycle (Moore et al., 2008), but also a major source of nutrients (e.g. Krest et al., 2000), trace metals (e.g. Windom et al., 2006) and radionuclides (e.g. Garcia-Orellana et al., 2013) to the coastal ocean. There are many approaches to quantifying SGD; hydrological models or balances (e.g. Pluhowski and Kantrowitz, 1964), direct measurements via seepage meters (e.g. Cable et al., 1997) and chemical tracers such as ^{222}Rn (e.g. Burnett and Dulaiova, 2003) or Ra isotopes (e.g. Moore, 1996) all have been used. Several models or approaches have been used to determine the amount of SGD by using Ra isotopes in coastal environments such as lagoons, bays, estuaries or open coastal areas: Ra mass balance (Moore, 1996; Krest and Harvey, 2003), Ra endmembers mixing model (Charette and Buesseler, 2004; Garcia-Solsona et al., 2010), eddy diffusion coefficient (Moore, 2000) and modeling (Turner et al., 1997; Robinson et al., 2007; Garcia-Orellana et al., 2010). The approach to quantifying SGD through a mass balance for Ra isotopes requires a detailed evaluation of both sources and sinks of Ra in the system. Sources of Ra include desorption from suspended riverine sediments, regeneration and release from bottom sediments, and input associated with submarine groundwater discharge (Moore, 1997; Hancock et al., 2000; Kelly and Moran, 2002). In locations with extensive marshland, tidal pumping and percolation of water through marsh sediments can also be a significant source of Ra, mainly short-lived isotopes, to the embayment (Bollinger and Moore, 1984; 1993). Ra is lost from the system principally in association with tidal exchange through inlets and by radioactive decay. The latter term is particularly important for the short-lived Ra isotopes (^{223}Ra and ^{224}Ra) and usually less important for the long-lived (^{228}Ra and ^{226}Ra). Previous studies involving mass balances of ^{223}Ra and ^{224}Ra in coastal systems have shown that diffusive inputs and desorptive losses from sediments are often small, and the dominant terms in the Ra balances are supply with SGD, exchange with the open ocean and decay (e.g., Charette et al., 2003; Beck et al., 2007, 2008; Garcia-Solsona et al., 2008a). However in estuaries with significant areas of muddy sediments and in which the water column is seasonally hypoxic, the flux of short-lived Ra isotopes from the sediments can be significant.

In this work we present the Ra mass balance used to evaluate the importance of the submarine groundwater discharge (SGD) in Long Island Sound (NY, US), a major "urban" estuary located in the northeastern USA, and affected by summertime hypoxia in the western basin.

2. SETTING

Long Island Sound (LIS) is the third most important estuary in US and it is located between Long Island (NY) and Connecticut (Fig. 1a). The dimensions are 93 km length and 34 km width with $6.2 \cdot 10^{10}$ m^3 of water volume and $2.8 \cdot 10^{9}$ m^2 of surface sediment. It ranges geographically from the East River in New York City to The Race at its eastern end, with an average depth of 20 m and with a salinity range between 23 and 31. The dominant freshwater input is from the Connecticut River, near the Sound's eastern end. Tidal ranges in LIS differ from west to east. In the western Sound the range is 2 – 3.5 m, whereas the range is smaller along the eastern shores (0 – 1 m). Tidal currents are strong in LIS, exceeding 1 m s^{-1} in the East River – a tidal strait connecting western LIS to the lower Hudson River – and range from ~5 m s^{-1} in the central basin to 1 m s^{-1} at the eastern end (Blumberg and Pritchard, 1997; Vieira, 1990). However, mean circulation is fairly weak, approximately 0.1 m s^{-1} or less (Vieira, 2000).

Historically, bottom water dissolved oxygen (DO) decreases during summer in Long Island Sound (LIS), such that hypoxia (DO < 3.0 mg L^{-1}) persists in the East River and western Narrows (Parker and O'Reilly, 1991). This seasonal hypoxia is attributed to the combined effects of phytoplankton and bacteria on biochemical oxygen demand (BOD) coupled with maximum density stratification of the water column (Jensen et al., 1991; Lee and Lwiza, 2008).

Seasonal hypoxia in LIS can affect trace element distributions. For example, Mn (IV) is used as an alternate electron acceptor in the bacterial oxidation of organic matter. Its reduction to the more soluble Mn(II) typically takes place in the muddy sediments of LIS, but under hypoxic conditions in the western Sound, the Mn "redoxcline" moves to the sediment water interface or even into the bottom water, resulting in an enhanced flux of dissolved Mn^{2+} into the water column. As this Mn^{2+} mixes and contacts oxic water, it is oxidized to Mn^{4+}, resulting in increased concentrations of particulate Mn. Thus, benthic Mn^{2+}(aq) fluxes vary seasonally in LIS and are higher in the summer than winter/spring (Aller, 1994).

Manganese oxide serves as an effective scavenger of radium. Thus under oxic sediment conditions, zones of Mn oxides in muddy sediments may act as a control on the Ra diffusive flux (Cochran, 1979; Torgersen et al., 1996). Conversely, reduction and solubilzation of Mn^{4+} as Mn^{2+}(aq), may release associated Ra into sediment pore water or overlying water and augment the flux of radium, especially short-lived, from the sediments due to diffusion and bioirrigation.

We hypothesize that in coastal environment such as Long Island Sound where the SGD is mainly governed by recirculation of overlying water through the sediments and seasonal hypoxia develops, seasonal variations of the ^{224}Ra inventories in the estuarine water column are related to hypoxia-driven cycling of manganese in the sediments as well as changes in bioirrigation by the benthic fauna. These processes must be evaluated in order to determine the contribution of SGD to the ^{224}Ra balance.

3. METHODS

Samples were obtained from stations in Long Island Sound (LIS) aboard the R/V *Seawolf* during spring (24 – 30 April) and summer (29 July – 04 August) 2009, and summer (03 – 12 August) 2010. Stations were oriented along 4 transects: one axial extending from the Narrows to the Race and three cross-Sound transects in the western, central and eastern Sound (Fig. 1b; Table S1 - Supplemental Data).

3.1 Water sampling and procedures

Water samples comprising 60 L of seawater were acquired at two depths – surface and deep – for every station. Surface samples were obtained with a submersible pump at approximately 0.5 m; deep samples were taken with Niskin bottles attached to the ship's rosette and tripped ~1 m from the bottom. A CTD was deployed at each station to determine profiles of temperature, salinity, and dissolved oxygen (DO). These water samples were stored in triple-rinsed plastic carboys. The 60 L water samples were subsequently filtered on-board through cartridges containing ~15 g Ra-adsorptive MnO_2-impregnated acrylic fiber (Mn-fiber), with untreated fiber acting as a pre-filter to eliminate particles. ^{223}Ra and ^{224}Ra were measured using a Delayed-Coincidence Counter (RaDeCC; Moore and Arnold, 1996; Garcia-Solsona et al., 2008b). Following counting of the Mn fiber in the RaDeCC, the fiber was leached in HCl and Ra was co-precipitated with $BaSO_4$. The $BaSO_4$ was removed from the leachate by centrifugation and sealed in glass vials for counting on a Canberra Intrinsic Ge well detector.

Counting efficiencies for the 352 keV ^{214}Pb (^{226}Ra) and 911 keV ^{228}Ac (^{228}Ra) peaks were determined using the IAEA 300 Baltic Sea Sediment Standard.

A second set of surface and deep samples was also obtained for suspended particle matter (SPM), Al(s), Mn(s) and Mn(aq) determination. Surface samples were taken with a Rubbermaid® HDPE 14-liter bucket lowered over the side of the ship; deep samples were taken from Niskin bottles. For SPM, 500 mL of each sample was transferred to an acid-washed Nalgene® 500-mL LDPE bottle and stored in the dark. In the laboratory, samples were vacuum-filtered through pre-weighed Whatman® Nuclepore membrane filters. Filters were dried and re-weighed. After SPM determination, filters were then transferred to acid-washed Falcon® Blue MaxTM 15-mL polystyrene conical tubes where 10 mL 6 N trace metal grade (TMG) HCl was added, the samples were vortexed, and leached for ~12 hours. Samples were then centrifuged at 3,500 – 4,000 rpm for ~20 min and supernatant transferred to acid-washed Wheaton® 8-ml HDPE bottles. All Mn(s) and Al(s) analyses were done on a Perkin-Elmer AAnalyst 800 atomic absorption spectrometer equipped with graphite furnace (GFAAS), employing Zeeman background correction. For Mn(aq), 30 mL of each water sample was filtered through a Whatman® PuradiscTM 0.2 µm PES filter (Cat. No. 6780-2502), acidified to 1.2 N with TMG concentrated HCl, and stored in acid-washed Nalgene® 30-mL HDPE bottles.

3.2 Sediment sampling and procedures

Sediment cores were taken at stations 8, 13, 16, and 120E (Fig. 1b) using a Soutar-type box corer (25 cm × 25 cm). ST13 and ST120E cores were taken on 29 July 2009 and ST8 and ST16 cores were taken on 09 August 2010 and 12 August 2010, respectively. A core also was collected by hand from a shallow, muddy sand station in Stony Brook (West Meadow Beach) on 24 July 2009.

For the LIS cores collected in 2010, two box cores were taken at each station. From one box-core, a subcore (9.5 cm diameter) was taken by pushing a butyrate acetate tube into the sediment, two subcores (7.5 cm diameter) were taken in the same manner, and a rectangular subcore was taken for x-radiography. From the other box core, one large subcore (20 cm diameter) was taken for measurement of $^{224,223}Ra$ fluxes. In 2009, only the large 20-cm diameter subcores were taken from a singe box core at each station. All subcores were 10 – 20 cm in length.

3.2.1 Ra flux Ra-flux incubations were carried out using the 20 cm-diameter subcores (modified Nalgene® polycarbonate multipurpose jars). The cores were covered with between 2.6 and 2.9 L of overlying Ra-free water from the bottom water taken at each site. For all cores (2009 and 2010) Ra fluxes were determined under oxic conditions by aerating the overlying water and circulating it continuously *via* a peristaltic pump connected to an in-line cartridge filled with ~15 g of Mn-fiber, following the scheme of Rodellas et al. (2012). At intervals ranging from 0.5 – 3 days, the cartridge was removed and the fiber was analyzed for ^{223}Ra and ^{224}Ra by delayed-coincidence counting methods (‘RaDeCC,’ Moore and Arnold, 1996; Beck et al., 2007). Ra concentrations were determined five times over the first ~250 hours after core collection under these aerated conditions. At the conclusion of the experiment, the cores were sectioned in 5 cm intervals and pore water was separated from the sediment by centrifugation. ^{224}Ra was measured in the pore water samples according to the methods described above.

For cores collected in 2010, we attempted to simulate the transition from summer oxic to hypoxic conditions and determine the effect on the ^{224}Ra flux. We began the hypoxic phase by bubbling N_2(g) into the overlying water of the core, which continued to circulate through Mn fiber and back into the core. However, in order to extract the diffused Ra onto Mn fiber (which is not stable under low oxygen conditions), the water was circulated through a reservoir that aerated it before it passed through the fiber. The water then circulated through a de-aeration reservoir and back into the core. It proved difficult to balance the aeration and de-aeration reservoirs to maintain a constant volume of overlying water in the flux core and to maintain very low dissolved oxygen in the water (values ranged from 2-3 mg·L^{-1}), and this approach was discontinued after two days. After that point, the flux cores were filled with de-aerated Ra-free LIS bottom water from the respective station, sealed, and the overlying water was continuously circulated with a magnetically coupled stirrer modified from the methods of Mackin and Swider (1989) and Aller (1994). Dissolved oxygen in the overlying water during this period was <1.5 mg·L^{-1}. At intervals ranging from 1 – 3 days, the overlying water of the flux core was carefully removed (and immediately replaced with de-aerated Ra-free water for the next flux measurement), aerated, filtered through Mn-fiber, and analyzed for ^{224}Ra by RaDeCC.

^{224}Ra fluxes under oxic conditions were estimated by plotting ^{224}Ra concentrations (dpm L^{-1}) vs time and determining the slope of the best-fit line. The slopes were multiplied by the overlying water volume and divided by the surface area of the polycarbonate containers to obtain fluxes in dpm m^{-2} d^{-1}. For the 2010 cores in which we tried to simulate the transition from summer oxic-to-hypoxic conditions, individual fluxes for each time point were calculated using equation (1):

$$J_{Ra} = \frac{C_{Ra(\Delta t)} \cdot V}{A \cdot \Delta t} \tag{1}$$

where $\boldsymbol{J}_{\mathbf{Ra}}$ = sediment Ra flux (dpm m^{-2} d^{-1}), $C_{\mathrm{Ra}(\Delta t)}$ = Ra concentration after time Δt (dpm L^{-1}), V = volume of the core overlying water (L), A = surface area of the core (m^2), and Δt = interval over which Ra is collected on the Mn fiber in oxic incubations or in which Ra is allowed to accumulate in overlying water during the hypoxic phase (d).

3.2.2 Mn(aq) flux. Incubations to determine the flux of Mn(aq) from the sediments were carried out in the 9.5 cm-diameter cores collected at stations 8 and 16 in 2010, adding as overlying water ~700 mL of unfiltered LIS bottom water (collected in a Niskin bottle) from the respective station. Two flux cores from each station were incubated in the dark at an *in situ* summer temperature of 21 ºC. The overlying water in one subcore was continuously circulated to ensure aeration; the other was sealed and continuously circulated with a magnetically coupled stirrer according to the methods of Mackin and Swider (1989) and Aller (1994). These subsequently will be referred to as "summer oxic" and "summer hypoxic" Mn flux cores respectively. At the close of these initial incubations, the summer hypoxic Mn flux cores from each station were moved to a dark cold-room set to an *in situ* winter temperature of 2.5 ºC and allowed to acclimate for 24 hours. After acclimation the seal was broken in order to allow gradual re-oxygenation. These are referred to as "winter oxic" Mn flux cores.

For all Mn flux core incubations a time series of multiple overlying water samples were extracted into syringes at 6-hour intervals during, at least, the first 24 hours then at various intervals thereafter based on observed DO. At each sampling time approximately 10 mL of overlying water was removed and simultaneously replaced with the aforementioned bottom water. Samples were passed through a Whatman® Puradisc™ 0.2 µm PES filter (Cat.

No. 6780-2502) and DO concentrations were determined via a modified Winkler titration method (Mackin et al., 1991). One hour later (after the modified Winkler titration was performed) another 9 ml was extracted and replaced. These samples were also filtered, acidified to 1.09 N with trace-metal grade (TMG) concentrated HCl, and analyzed for dissolved Mn(aq). The dissolved Mn concentrations in the overlying water of the flux cores were corrected for dilution due to replacement of seawater taken for DO measurements (dilution factors were variable in the different cores due to differences in core overlying water volumes). Because samples were passed through a 0.2 µm filter (thus excluding sediment), a correction for particulate Mn contribution to the "dissolved" Mn was not necessary. All Mn analyses were done on by GFAAS. Acidified seawater samples were diluted with de-ionized water and analyzed in triplicate to determine Mn(aq) concentrations (in mmol L^{-1}).

3.2.3 Sediment core solid phase analyses. The 7.5 cm-diameter subcores were sampled to obtain profiles of water content, organic matter content, and total leachable Mn. Cores were sectioned at 0.5 cm intervals to a depth of 3 cm, and at 1 cm intervals from 3 cm to a depth of 6 cm. Sections were dried at 60 ºC for 24 h to determine water content. The core sections were then pulverized to a powder with an agate mortar and pestle for the analyses. Sediment (~1.5 g) from each core section was combusted in a muffle furnace at 450ºC for 6 h and organic matter content determined by loss-on-ignition. Approximately 150 to 200 mg of dry sediment from each core section was leached with 10 mL 6 N trace metal grade (TMG) HCl for 24 hours in acid-washed Falcon® Blue Max™ 15-mL polystyrene conical tubes. Samples were then centrifuged at 3,500 – 4,000 RPM for ~20 min and the supernatant was transferred to acid-washed Wheaton® 8-mL HDPE bottles. Total leachable Mn and Al were determined via GFAAS.

Sediment from the Ra incubation cores was removed by sectioning each core in 1 cm intervals after the flux experiments were completed. The sediment was dried and ground and sealed into jars for measurement of ^{226}Ra, ^{228}Ra and ^{228}Th by gamma spectrometry with a 3800 mm^2 Canberra intrinsic Ge detector, using the gamma emissions at 352 keV (^{214}Pb), 911 keV (^{228}Ac) and 583 keV (^{208}Tl), respectively. Counting efficiencies were determined using the IAEA 300 Baltic Sea Sediment Standard and no self-absorption corrections were made due to the relatively high gamma energies.

3.2.4 X-radiographs. Rectangular subcores were stored in LIS water and aerated. Images were taken in the days immediately following coring with a digital x-ray setup.

4. RESULTS

4.1 Temperature, salinity and dissolved oxygen

Figure 4 shows the temperature, salinity and DO profiles in stations along the axial transects in spring (2009) and summer (2010). Table S1 (Supplemental Data) gives temperature, salinity and DO of the water column at the surface and bottom layers during the spring and summer sampling campaigns. During spring 2009, samples showed a gradient of temperatures and salinities from The Race (ST 101) to the East River (ST 16) ranging from a mean temperature of 6.4 and 9.9 ºC and from a mean salinity of 30.5 and 25.6, respectively. The distribution of DO in each station along LIS is constant with a mean value of 9.9 $mg \cdot L^{-1}$, except for ST 16 in the western Sound that was likely influenced by exchange with the East River. Temperature and salinity showed relatively constant profiles in the spring, with a slight decrease of temperature with depth for the eastern stations and an increase of salinity with depth in The Race station (ST101).

During summer 2010, profiles showed that the water column was divided into two major layers: a surface layer with high temperature, lower salinity and a deeper layer with lower DO. These two layers were separated by a well-developed pycnocline layer. The surface layer (0-6 m to 0-9 m) was homogenous with a temperature ranging from 22.8 to 23.7 ºC, salinity between 23.2 and 26.3 and DO from 2.8 to 7.1 mg·L^{-1}. The dense bottom layer occurred from 6-10 m to the bottom, depending on which parameter (T, S or DO) was considered. Temperature showed the thermocline between 6 and 8 m with bottom temperatures ranging from 19.5 and 22.9 ºC from east to west. A halocline was evident from 6 to 10 m; bottom water salinities ranged between 26.6 and 30.3 with a gradient from west to east. Finally, the oxycline occurred between 8 and 12 m, with concentrations in bottom waters ranging from 2.7 and 6.7 mg·L^{-1}. DO showed a clear decrease in concentration from The Race to East River in agreement with previous studies (Parker and O'Reilly, 1991; Anderson and Taylor, 2001; Lee and Lwiza, 2008)

4.2 Ra activities in LIS

^{224}Ra was well correlated with ^{223}Ra for virtually all samples from LIS (Fig. S1 Supplemental Data); therefore subsequent discussion of the distribution of short-lived Ra in LIS is focused on ^{224}Ra because data are more complete and precise. ^{224}Ra activities along the central transect were generally greater in the deep water than surface samples in all seasons (Fig. 3; Table S2 - Supplemental Data). Summer 2009 and 2010 data showed markedly higher ^{224}Ra activities than spring 2009 with a general pattern of higher ^{224}Ra in the western Sound and greater activities in deep samples (Fig. 3; Table S2 - Supplemental Data). Mean ^{224}Ra activities of 10.9 ± 4.2 dpm·100L^{-1} in summer 2009 and 2010 were more than 2-fold higher than the average concentration of 5.4 ± 1.3 dpm·100L^{-1} in spring 2009 (Table 1).

^{224}Ra activities along the three cross-Sound transects in the western, central and eastern Sound in spring 2009 and summer 2010 do not show a clear trend in spring 2009, but in summer 2010 showed higher activities in stations close to the Connecticut and Long Island shores (Fig. 4; Table S2 - Supplemental Data), in agreement with the previous results of Torgersen et al. (1996) and Bokuniewicz et al. (submitted). Thus, the inventory of ^{224}Ra in the water column in summer was two times higher than in spring, indicating an increased ^{224}Ra flux to the Sound in summer (Table 3).

Although the data are not as extensive as those for ^{224}Ra, measurements of ^{226}Ra and ^{228}Ra activities along the central LIS transect showed seasonal differences, especially for ^{228}Ra, similar to those of ^{224}Ra (Fig. 5; Table S2 - Supplemental Data). Mean activities for ^{226}Ra were 9 ± 3 dpm·100L^{-1} in spring 2009 and 11 ± 2 dpm·100L^{-1} for both summer samplings (2009 and 2010). ^{228}Ra showed a larger seasonal difference, with a mean of 42 ± 13 dpm·100L^{-1} in spring 2009 and 66 ± 25 and 74 ± 19 dpm·100L^{-1} for summer 2009 and 2010, respectively. These values are comparable to those obtained by Turekian et al. (1996) in summer 1991 and 1993: 16 ± 3 and 14 ± 2 dpm·100L^{-1} for ^{226}Ra in 1991 and 1993, respectively, and 65 ± 13 dpm·100L^{-1} for ^{228}Ra in 1991.

4.3 Suspended particulate matter (SPM)

Suspended particle concentrations were similar in surface and deep water in spring 2009 with a mean concentration of 1.5 ± 1.3 mg·L^{-1}. In summer 2010, SPM concentrations were generally higher (mean 3.3 ± 2.3 mg·L^{-1}) than in spring 2009 and had higher concentrations in deep samples (mean 4.7 ± 2.6 mg·L^{-1}) and a clear increasing gradient of SPM from east to west in summer 2010 with maximum concentration of 13.5 mg·L^{-1} at ST16 (Table S1 -

Supplemental Data). SPM concentrations were comparable to the previous results of Kim and Bokuniewicz (1991).

4.4 Dissolved and particulate Mn

Dissolved Mn concentrations (Mn_{aq}) were similar in spring 2009 throughout LIS with lower concentrations in the central than in the western Sound and lowest concentrations at the Race (Fig. 6). Summer 2009 Mn_{aq} were highest in deep samples throughout the Sound with the exception of ST16 in the Narrows (Fig. 6). Compared with spring 2009, summer 2009 deep Mn_{aq} concentrations within the western Sound were higher, and surface concentrations throughout LIS were lower, with the exception of ST16 (Fig. 6). Summer 2010 Mn_{aq} concentrations followed the pattern of summer 2009, but showed higher concentrations: western LIS values were 168% higher than spring 2009 values and deep sample concentrations in the central and eastern Sound were 158% higher than surface Mn_{aq} (Fig. 6). Overall, the 2010 data showed a general pattern of elevated deep Mn_{aq} concentrations compared with those in surface waters and highest values in the western Sound and along the Sound margins (Fig. 6; Table S1 - Supplemental Data).

Particulate Mn (Mn_p) concentrations in spring and summer 2009 showed no clear trends. Summer 2010 data showed a pattern of elevated surface Mn_p concentrations relative to deep with highest values occurring in the central Sound (Fig. 6).

4.5 Core incubations

4.5.1 Ra fluxes.

The ^{224}Ra fluxes from the sediment incubations under oxic, well-mixed conditions are summarized in Table 2 (see also Fig. S2- Supplemental Data). Taking the two years as a single set, the ^{224}Ra fluxes under fully aerated, summer temperature conditions displayed the following relationship among the stations: $J_{Ra}^{ST13} > J_{Ra}^{ST120E} > J_{Ra}^{ST8} > J_{Ra}^{ST16} > J_{Ra}^{STWM}$.

In the incubation cores from 2010 (from ST8 and ST16), the two cores displayed differences in Ra flux values, yet similar variations in flux with time as hypoxic conditions were imposed (Fig. 7). DO decreased from ~3 mg L^{-1} to less than 1.5 mg L^{-1} during the hypoxic phase. At ST8, ^{224}Ra fluxes decreased from the oxic phase flux (average 164 ± 13 dpm m^{-2} d^{-1}) to ~50 dpm m^{-2} d^{-1} for several days of hypoxic incubation (Fig. 7a). ^{224}Ra flux then increased for the following two incubation periods, first peaking at ~140 dpm m^{-2} d^{-1} for a 1-day incubation then decreasing to ~70 dpm m^{-2} d^{-1} for the final 2-day incubation (Fig. 7a).

A similar pattern was observed at ST16, although the hypoxic fluxes were higher (Figure 7b). Fluxes under oxic conditions were 127 ± 12 dpm m^{-2} d^{-1} and, under hypoxic conditions, initially decreased to ~75 dpm m^{-2} d^{-1}, ~60% of the oxic flux. Fluxes then increased to a maximum of 214 dpm m^{-2} d^{-1}, approximately twice the oxic value and then decreased to ~170 dpm m^{-2} d^{-1} but remained greater than the oxic flux (Fig. 7b).

4.6.2 Mn fluxes. Net dissolved Mn fluxes, $\boldsymbol{J_{Mn}}$ (mmol m^{-2} d^{-1}), were estimated according to equation (2), modified from Aller (1994).

$$J_{Mn} = \frac{\left[C_{Mn}(t) - C_{Mn}(t\text{-}\Delta t)\right] \cdot V(t)}{A \cdot \Delta t} \qquad (2)$$

where $C_{Mn}(t)$ = Mn(aq) concentration at time t (mmol L^{-1})

$C_{Mn}(t - \Delta t)$ = Mn(aq) concentration in the previous sample (mmol L^{-1}),

$V(t)$ = volume of the core overlying water (L),

A = surface area of the core (m^2),

Δt = change in time since the previous sample (d).

The summer oxic Mn flux cores maintained saturated concentrations of DO and Mn(aq) fluxes were small at both stations: ST8 showed fluxes less than 0.5 mmol m^{-2} d^{-1}, after an initial pulse (1.6 mmol m^{-2} d^{-1}, probably related to disturbance associated with core collection) and ST16 had negative fluxes (into the sediments) (Figure 8a and b).

The summer hypoxic Mn flux core for ST8 showed fluxes near zero until DO reached a value near 3.0 mg L^{-1} (Fig. 8c) after which the flux increased significantly over ~29 hours and then decreased slightly for the final two sampling times (Fig. 8c). As this core was allowed to transition to winter (2°C) oxic conditions, the DO increased rapidly and Mn was removed from the overlying water (Fig. 8c).

Simulation of summer hypoxic conditions at ST16 produced hypoxia within ~6 hours (Fig. 8) and more rapidly than for ST8 (~48 hours, Fig. 8d) – and the core displayed an immediate high Mn flux of 2.9 mmol m^{-2} d^{-1}, decreasing gradually thereafter (Fig. 8c). Establishment of winter oxic conditions produced Mn fluxes into the sediment, as at ST8 (Fig. 8d).

4.6.3 Sediment core physico-chemical analyses. Water content was almost identical between ST8 and ST16 and indicative of the muddy nature of the sediments (Table S3 - Supplemental Data). ST16 had a slightly greater percentage of organic matter in the top 0.5 cm of sediments than ST8; the same pattern emerged at sediment depths below 3.0 cm (Table S3 - Supplemental Data). Sediment Mn concentrations were more than two-fold higher in the top 0.5 cm at ST8 than ST16. Below 1 cm, both subcores exhibited similar Mn concentrations, although concentrations decreased gradually with depth at ST8 and increased gradually with depth at ST16 (Table S3 - Supplemental Data).

The solid phase radionuclide measurements (Table S4 - Supplemental Data) showed comparable activities of the ^{232}Th series nuclides at all the sites. The pore water ^{224}Ra activities were ~10 times greater than those in the overlying water and show relatively little variation with depth (Table S5 - Supplemental Data).

4.6.4 X-radiographs. Benthic infaunal organism abundances were higher at ST16 than ST8 due to the greater number of burrows and remnant shell (Fig. S3 - Supplemental Data). However, structure and actual abundances may differ because the former can integrate over time.

5. DISCUSSION

5.1 Dissolved oxygen, manganese and ^{224}Ra activities

DO in LIS during spring 2009 was uniform in surface and deep samples except in the Narrows where surface DO concentrations were 14% and 21% higher compared with bottom waters at ST16 and ST13, respectively. During summer 2009 and summer 2010, DO values were not only lower overall compared with spring, but lower in deep samples than in surface samples (Table S1 - Supplemental Data). The disparity between surface and deep DO values during summer can be attributed to stratification of the water column, which occurred in the central Sound (Fig. 2) and caused DO-depletion to be localized below the pycnocline. During summer 2010, the extreme western Narrows (ST16) showed little to no stratification and uniformly hypoxic or near-hypoxic conditions. The absence of stratification there resulted in DO-depletion throughout the water column.

Both deep $Mn_{(aq)}$ and deep ^{224}Ra were strongly correlated with DO concentrations in LIS during summer 2010 (Fig. 9a and b). ^{224}Ra concentrations were greatest during summer sampling periods in regions of the LIS with low DO concentrations. In summer 2009 and 2010 in stations where hypoxia occurred, Ra showed a general pattern of higher deep concentrations than surface concentrations, especially in the central and eastern Sound (Fig. 3). Stations nearest the Connecticut and LI shores showed less difference in surface and deep concentrations, presumably due to shallower water and enhanced input of ^{224}Ra along the Sound margins (Fig. 4; Torgersen et al., 1996). ST18 and ST16 in the western Narrows exhibited little or no stratification, thus Ra concentrations were high in both surface and deep water (Fig. 3a and b).

$Mn_{(aq)}$ concentrations also were highest during summer sampling periods in the western LIS (Fig. 6). Furthermore, a pattern of higher deep $Mn_{(aq)}$ concentrations in the central LIS was evident during summer 2009 and was observed again during summer 2010 (Fig. 6). This is in agreement with the seasonal pattern of Mn redox cycling observed by Aller (1994). $Mn_{(aq)}$ concentrations in the western LIS were more uniform throughout the water column presumably due to a greater reductant C_{org} flux and low DO. The relationships among dissolved manganese, ^{224}Ra and DO suggest that the presence of a manganese oxide "redox barrier" in the sediments can have a significant effect on the ^{224}Ra flux to the overlying water. Sun and Torgersen (2001) modeled this effect and showed that ^{224}Ra was effectively scavenged by manganese oxides within the sediments of LIS.

5.2 The mass balance of ^{224}Ra in LIS

When SGD is quantified by difference using a Ra mass balance, all other sources of Ra must be accurately determined. Radium inputs to LIS include desorption from riverine sediments entering and Sound and from resuspended sediments, the flux from bottom sediments, exchange with the sea and New York Harbor and the input associated with SGD. On the other hand, radium is lost from the system principally by radioactive decay of the short-lived Ra isotopes (^{223}Ra and ^{224}Ra) and the exchange with low-Ra seawater through inlets.

5.2.1 Seawater exchange

Long Island Sound is connected with the Atlantic Ocean (Block Island Sound) via The Race (ST101). The sample collected in spring 2009 at ST101 showed the lowest ^{224}Ra activity of all the sampling stations, 3.6 dpm·100L^{-1}. This value is lower than those reported by Torgensen et al. (1996) in the same area ($^{224}Ra_{surf}$= 8.9 dpm·100L^{-1} and $^{224}Ra_{deep}$= 12.9 dpm·100L^{-1}) and those reported by Beck et al. (2008) for the mouth of Great South Bay (14.4 dpm·100L^{-1}, although this value was likely influenced by recirculated bay water).

Fluxes of water in and out of LIS through the Race were determined by Crowley (2005) to be 5.92 ·10^{14} and 5.74 ·10^{14} L·y^{-1}, respectively. Given the ^{224}Ra activity for The Race (^{224}Ra= 3.60 ± 0.22 dpm·100L^{-1}) and the average Ra activities in the eastern Sound for spring 2009 (5.95 dpm·100L^{-1}) and summer 2009 and 2010 (7.30 and 7.18 dpm·100L^{-1}, respectively), the ^{224}Ra flux into LIS from Block Island Sound is (21.3 ± 1.4)·10^{12} dpm y^{-1} (assumed comparable for both spring and summer) and the fluxes from LIS to Block Island Sound are (34.2 ± 8.0)·10^{12} and (41.6 ± 16.0)·10^{12} dpm y^{-1} for the spring and summer, respectively (Table 4).

5.2.2 East and Connecticut Rivers

The two main rivers that supply freshwater to the LIS are the Connecticut and the East Rivers. Estimated freshwater from the Connecticut River is 1.7·10^{13} L·y^{-1} (Dion, 1983). The ^{224}Ra activities of the Connecticut River (ST4) for spring 2009 and summer 2010 were 8 ± 1 and 12 ± 4 dpm·100L^{-1}, respectively, yielding ^{224}Ra fluxes of (1.4 ± 0.1)·10^{12} and (2.0 ± 0.4)·10^{12} dpm y^{-1} to LIS. Because ST4 is near the mouth of the Connecticut River and its salinity is high enough (~ 28) to guarantee the total desorption of Ra isotopes from suspended particles, these fluxes include both dissolved ^{224}Ra and desorption of ^{224}Ra from riverborne particles.

The East River serves as the western boundary of LIS and acts as an estuary with exchange between LIS and New York Harbor. The flux of water from the East River to LIS is 4.6·10^{13} L·y^{-1} and that from LIS to East River is 6.4·10^{13} L·y^{-1} (Robert Wilson, personal communication). The ^{224}Ra activity determined for the East River is 9 ± 2 dpm·100L^{-1} (data not shown). Therefore the ^{224}Ra flux from the East River into LIS is (4.1 ± 0.9)·10^{12} dpm·y^{-1}. Mean activities for ^{224}Ra in the deep water of western LIS are 6.9 ± 1.3 dpm·100L^{-1} and 18.2 ± 4.5 dpm·100L^{-1} for spring 2009 and summer 2010, respectively. If we assume estuarine circulation associated with the East River-LIS and use these activities to determine the flux of ^{224}Ra from LIS to NY Harbor via the East River, we obtain (4.4 ± 0.8)·10^{12} and (11.6 ± 2.9)·10^{12} dpm y^{-1} for spring 2009 and summer 2010, respectively.

5.2.3 Desorption from resuspended particles

^{224}Ra also may be added to the water column through desorption from resuspended bottom sediments. The short half-life of this isotope ensures a rapid production from decay of ^{228}Th on and in the bottom sediments. Our measurements of ^{224}Ra in sediment pore water (0-2 cm) after the incubation experiments (Table S5 - Supplemental Data) gave values of ~15 dpm·L^{-1}. The K_d of Ra in the fine-grained sediments of LIS is ~50 L·kg^{-1} (Cochran, 1979; Sun and Torgersen, 1980). Thus, the adsorbed ^{224}Ra at the sediment-water interface is ~0.75dpm·g^{-1}. This radium can be desorbed as the surface sediments are resuspended into the overlying water column (with relatively low particle concentrations compared with the solid/pore water ratio in bottom sediments). Resuspension rates for the muddy sediments of LIS can be estimated from our measured suspended sediment concentrations, with the assumption that resuspension is tidally-mediated and thus occurs on a time scale of 0.5 d. The measured suspended sediment concentrations of 1.5 ± 1.3 $mg \cdot L^{-1}$ for spring and ~4 ± 2.5 $mg \cdot L^{-1}$ for summer give standing crops of 3 ± 2.6 $mg \cdot cm^{-2}$ in the spring and 8 ± 5 $mg \cdot cm^{-2}$ in the summer for an average depth of LIS of 20 m, and the resuspension fluxes required to support these standing crops are thus 6 ± 5.2 $mg \cdot cm^{-2} \cdot d^{-1}$ and 16 ± 10 $mg \cdot cm^{-2} \cdot d^{-1}$. Sediment fluxes measured in sediment traps in LIS showed a similar seasonal variation (McCall, 1977) but are generally greater than our estimates (~70 $mg \cdot cm^{-2} \cdot d^{-1}$ in summer; Bokuniewicz et al., 1991; 121 ± 11 and 250 ± 15 $mg \cdot cm^{-2} \cdot d^{-1}$ in spring and summer, respectively; McCall, 1977). However, the traps in both studies were deployed close to the sediment-water interface–10-30 cm in the case of McCall (1977) and 1 m in the case of Bokuniewicz et al. (1991) –and difference in fluxes in the two studies likely reflects this. We view these values as not representative of the fluxes required to support the observed suspended sediment concentrations in the water column of LIS and thus likely to release desorbed ^{224}Ra through the water column.

If the sediment pore water ^{224}Ra is at steady state, such that tidal resuspension of sediment continuously supplies desorbable ^{224}Ra to the water column, and if desorption is rapid and is dominated by the fine-grained sediment characteristic of the western and central basins of LIS (~67% of the total area), we calculate ^{224}Ra fluxes of $(31 \pm 27) \cdot 10^{12}$ $dpm \cdot y^{-1}$ for the spring and $(82 \pm 51) \cdot 10^{12}$ $dpm \cdot y^{-1}$ for the summer (Table 4). These fluxes are maximum estimates because, in addition to the assumptions given above, they assume that all the filterable particles in the water column of LIS are derived from resuspended bottom sediments and so neglect in situ production of biogenic particles. The continual input of Ra derived from desorption from resuspended particles should not be as important for the long-lived radium isotopes (^{228}Ra and ^{226}Ra) because regeneration of desorbable Ra is dependent on their half-lives and is thus slow relative to resuspension driven by the tidal circulation in the Sound.

5.2.4 Decay

Radioactive decay at steady state is estimated easily considering the ^{224}Ra inventory in LIS and the decay constant of ^{224}Ra. The inventory is calculated from the average radium activities in the surface and deep water samples in each basin (eastern, central and western) and the volume in the corresponding area (Table 3). During the sampling periods, decay term were $(205 \pm 34)\cdot 10^{12}$ $dpm\cdot y^{-1}$ for spring 2009 and $(447 \pm 88)\cdot 10^{12}$ $dpm\cdot y^{-1}$ for summer 2010 (Table 4).

5.2.5 Sediment diffusion and bioirrigation

The flux of ^{224}Ra from the sediments of LIS is a potentially important source of Ra to the overlying water. As ^{224}Ra is produced in the sediments from ^{228}Th decay, a portion of the produced Ra atoms are recoiled into the pore water. As noted above, they can adsorb onto particle surfaces and be desorbed during resuspension. Dissolved Ra atoms are also able to diffuse through the pore water and are subject to bioirrigation that facilitates transport into the overlying water column. Although bioirrigation involves fluid flow across the sediment-water interface, this processes is excluded from the definition of SGD (Moore, 2010b) and we treat it separately in constructing the ^{224}Ra balance.

Our oxic core incubation data show that the ^{224}Ra flux mediated by diffusion and bioirrigation is readily measurable in the laboratory over short time periods. To incorporate this flux into the Ra mass balance requires estimates of fluxes under both spring and summer conditions. Incubations were run under temperatures closer to summer (20 °C) and with fully oxic overlying water. Under these conditions, the benthic faunal community is active and the Mn redox barrier to Ra diffusion is present within the sediment. Thus these represent summer conditions that might be expected in central and eastern LIS, which generally have an oxic water column during the summer. The cores from central LIS have oxic ^{224}Ra fluxes of 164 ± 13 (ST8) and 170 ± 7 (ST120E) dpm m^{-2} d^{-1} and 57 ± 3 dpm m^{-2} d^{-1} in the sandy mud core from West Meadow (Table 2).

Although the temperature was maintained at 20 °C throughout the experiment, the incubation cores from 2010 can be used to obtain some idea of the magnitude of the ^{224}Ra flux from the sediments at other times of the year and under other conditions. Following the oxic incubation, the cores were allowed to become hypoxic. Initially the DO dropped to only ~3 mg·L^{-1}. Bioirrigation was suppressed, but the data from the Mn flux cores (Fig. 8) suggest that Mn had not yet been reduced and mobilized. The ^{224}Ra flux in both cores decreased to ~50 - 75 dpm m^{-2} d^{-1} (Fig. 7). This likely represents the flux of ^{224}Ra without bioirrigation, but with the Mn redox barrier in place. Indeed, a comparable flux (~50 dpm m^{-2} d^{-1}) may be calculated using Fick's first law applied to the pore water ^{224}Ra data obtained for the 2009 cores at the end of the oxic incubations (Table S5 - Supplemental Data).

During the next phase of the hypoxic incubations in the 2010 cores, DO decreased to ~1 mg·L^{-1} and the ^{224}Ra flux increased in both cores. We attribute this pattern to the reduction of Mn^{4+} in the sediment and release of associated ^{224}Ra. Fluxes then decreased, but in the core from western LIS (ST16) remained elevated above those observed during the oxic incubation (Fig. 7), likely due to the absence of the Mn redox barrier.

We have translated this pattern into a seasonal approximation of the ^{224}Ra flux from LIS sediments as follows. We divide LIS into three sections: western, central and eastern (Fig. 1b). The central and eastern regions experience minimal if any seasonal hypoxia and the principal difference between them is the sediment type, with muddy sediments in the central basin and sandy sediments in the eastern. We assume that the principal seasonal difference in the ^{224}Ra flux in these areas is caused by variation in benthic faunal activity producing bioirrigation (Cai et al., 2013), and that this process tracks water temperature (REF). We take the minimum ^{224}Ra flux observed under mildly hypoxic conditions (~50 dpm m^{-2} d^{-1}) as reflecting the absence of biorirrigation under conditions typical of the winter, and consequently a ^{224}Ra flux dominated by molecular diffusion. In contrast, ^{224}Ra fluxes of ~167 dpm m^{-2} d^{-1} (the average of ST8 and ST120E) and ~57 dpm m^{-2} d^{-1} (the value for the sandy core STWM), can be taken as representative of conditions of maximum bioirrigation and summer conditions for the central and eastern Sound, respectively. Using the seasonal temperature trend in LIS (Aller, 1977), we fit a 4th-order polynomial to the pattern including the "summer" and "winter" ^{224}Ra fluxes as defined above and determine the appropriate flux for our April and August samplings. For the eastern, sandy portion of LIS we scale the winter fluxes determined for the muddy sediments to that of the sandy core. These fluxes give the sediment Ra fluxes for our spring (April, 2009) and summer (August, 2009 and 2010) samplings: 100 and 160 dpm m^{-2} d^{-1} for central LIS and 35 and 55 dpm m^{-2} d^{-1} for the eastern sound, respectively.

For western LIS, which experiences strong summer hypoxia, we use the approach described above to scale the seasonal change in bioirrigation driven by water temperature, but use the pattern of DO and maximum ^{224}Ra fluxes observed in the incubation experiment with the core from ST16 to include higher short-term ^{224}Ra fluxes associated with low DO and Mn oxide reduction. This allows us to estimate fluxes for April and August for western LIS to use in the ^{224}Ra mass balance: 100 and 220 dpm m^{-2} d^{-1}, respectively. The area of LIS west of the Race (Fig. 1) is $2.8 \cdot 10^{9}$ m^{2}, and western, central and eastern sub-basins each comprise approximately 1/3 of the total. The resultant net fluxes of ^{224}Ra from the sediments of LIS (in dpm y^{-1}) are given in Table 4.

5.2.6 ^{224}Ra mass balance model and estimates of ^{224}Ra supplied by submarine groundwater discharge

Table 4 shows the ^{224}Ra mass balance for spring and summer periods in Long Island Sound. As all the Ra fluxes are determined, the Ra imbalance between inputs and outputs can be ascribed to SGD. Thus, the estimated ^{224}Ra-derived SGD fluxes are $(106 \pm 50) \cdot 10^{12}$ and $(244 \pm 112) \cdot 10^{12}$ $dpm \cdot y^{-1}$ for spring and summer conditions, respectively.

We have included estimates of errors in the calculation of ^{224}Ra supplied by SGD, but it is difficult to fully assess the uncertainties associated with all of the terms in the mass balance. The most significant terms in the ^{224}Ra balance are the loss by decay in the water column and gains from diffusion and bioirrigation in bottom sediments and desorption during sediment resuspension. Error in the decay term can be estimated as the uncertainties on the average ^{224}Ra inventories in LIS for the spring and summer samplings. These are of the order ±16-20% (Table 4).

The flux from bottom sediments is based on relatively few measurements (4 muddy cores from the western and central Sound, 1 sandy core), and using the standard deviation of the mean seems unjustified. In addition, as described above, we have scaled the fluxes according to temperature in the water for central and eastern LIS, and a composite of temperature and dissolved oxygen for western LIS. We assign an uncertainty of ±30% to the resultant fluxes. The release of ^{224}Ra by desorption from resuspended particles has uncertainties (~ ±60 – 90%) that are based on those associated with the average suspended sediment concentrations. The other terms in the ^{224}Ra mass balance are less important and their errors do not contribute significantly to the ^{224}Ra flux attributed to SGD (Table 4). Although the spring ^{224}Ra fluxes due to SGD are nominally less than those in the summer, the values overlap within the uncertainties.

5.2.7 Processes driving the SGD flux

The most accepted definition of SGD was provided by Burnett et al. (2003), who defined SGD as any flow of water out across the sea floor without regard to its composition (e.g., salinity), its origin, or the mechanism(s) driving the flow. Taniguchi et al. (2002) defined SGD as the addition of two components: SFGD defined as the submarine fresh groundwater discharge and the RSGD defined as the recirculated saline groundwater. Therefore, the estimated total net SGD in our ^{224}Ra balance comprises both net fresh groundwater and recirculated LIS water components.

Elevated ^{224}Ra concentrations in pore waters compared with surface (overlying) waters along the LIS shore, as seen in our cross-Sound transects and in shore samples reported by Bokuniewicz et al. (submitted), illustrate the process of Ra input from nearshore sandy sediments (Boehm et al., 2006). As seawater percolates through the beach face between tidal cycles, ^{224}Ra that accumulates in pore waters is transported to surface waters offshore (Urish and McKenna, 2004). Subsequent dilution occurs due to wave action and mixing over the course of the tidal cycle. A transect made in Smithtown Bay from the shore out into the open LIS demonstrates the importance of this process for adding ^{224}Ra to LIS

(Bokuniewicz et al., submitted). Values decreased from ~55 dpm $100L^{-1}$ nearshore to ~15 dpm $100L^{-1}$ at 2 km offshore and decreased further to ~5 dpm $100L^{-1}$ in the open Sound (ST120E). Salinity increased from ~24 to 26 over the same transect (Bokuniewicz et al., submitted).

The tidally-mediated flux of water through beach sands is a form of submarine groundwater discharge *sensu* Burnett et al. (2003). The short half-life of ^{224}Ra ensures that it is produced rapidly in the beach sediments and mobilized to the pore water via recoil. Indeed we are able to confirm that production of ^{224}Ra over a tidal cycle can account for the observed activities. We collected a core from Smithtown Bay and isolated it with pore water for several weeks, long enough for ^{224}Ra to reach a steady state between production and decay. The steady state pore water activity was 1100 ± 26 dpm $100L^{-1}$. The water entering the sediment on high tide had 60 dpm $100L^{-1}$ and the water seeping out of the beach face as the tide was receding had 174 dpm $100L^{-1}$. Using a simple equation of ingrowth balanced by decay, the time to produce the difference between the incoming and outflowing water is ~0.6 d, consistent with a tidal cycle (Bokuniewicz et al., submitted). Thus, the LIS nearshore data demonstrate a marginal input of ^{224}Ra to LIS, especially in areas comprising sandy sediments. This conclusion is in agreement with that of Torgersen et al. (1996), who found that the distribution of surface ^{224}Ra in LIS was a function of cross-Sound (N – S) distance and eddy dispersive mixing.

Boknuiewicz et al. (submitted) modeled the distribution of ^{224}Ra along a transect extending from 1 m water depth nearshore to central LIS. The ^{224}Ra flux per meter of shoreline required to support the distribution was $1.03 \cdot 10^8$ dpm m^{-1} y^{-1}. Extrapolating to the shoreline lengths of the Long Island and Connecticut shores of LIS (Bokuniewicz et al., submitted) yields ~98 - 208 · 10^{12} dpm y^{-1}. This is quite comparable to the ^{224}Ra flux due to

SGD calculated from the ^{224}Ra mass balance (Table 4). We conclude that tidal percolation through the coarse-grained sediment along the Long Island shore can supply the ^{224}Ra attributed to SGD in the ^{224}Ra balance.

If the SGD flux of ^{224}Ra into LIS is caused principally by tidal percolation through coarse-grained sands along the shores of the Sound, there is no clear reason for this process to be seasonal and to be greater in the summer than in the spring, although other studies have also reported seasonal differences between winter and summer (e.g. Moore, 2010). Thus, seasonal differences in the ^{224}Ra balance, if real, must be attributed to other factors. The supply of ^{224}Ra from bottom sediments represents the second largest source of this radionuclide to the LIS water column. Our incubation experiments suggest that bioirrigation and Mn redox cycling, both of which vary seasonally in LIS, are important in controlling the ^{224}Ra flux from the bottom. It seems likely that our estimates of the ^{224}Ra flux from bottom sediments do not adequately represent spatial or seasonal variations in that source of ^{224}Ra to the overlying LIS water column, especially under summer hypoxic conditions. Moreover, the flux of ^{224}Ra during the summer as hypoxia develops is likely to be temporally variable, reflecting both the reduction of manganese oxides and release of associated Ra as well as changes in the flux from the bottom with reduced bioirrigation and the absence of a manganese redox barrier in the sediments. This implies that accurate balances for the short-lived Ra isotopes must take into account the importance of muddy sediments, especially in estuaries that experience seasonal hypoxia.

The ^{224}Ra SGD fluxes of 106 – 244 $\cdot 10^{12}$ dpm y^{-1} (Table 4) can be converted to a SGD flow by considering the ^{224}Ra activities of the water that is transferred out the coarse sediment due to SGD. Analyses of beach pore water reported in Bokuniewicz et al. (submitted) range from 120 to 680 dpm 100L^{-1} with a mean of 330 dpm 100L^{-1}. Therefore the volumetric flux of SGD is 32 - 74 $\cdot 10^{12}$ L y^{-1}.equivalent to 1.3 – 3.5 times the flux of fresh water delivered to LIS by the Connecticut River. This comparison agrees with other studies conducted in the western shore of the North Atlantic Ocean (e.g. Moore, 2010) or the entire Atlantic Ocean (Moore et al., 2008), that concluded that the total SGD flux is up to ~3 times greater than the river flux. Compared with the fresh groundwater underflow for Nassau and Suffolk counties estimated at $3.45 \cdot 10^{11}$ $L \cdot y^{-1}$ (Monti and Scorca, 2003), the SGD for LIS calculated from the ^{224}Ra balance is ~100 times that of the fresh SGD. In other words, recirculated seawater accounts for ~100% of the total SGD flow into LIS.

5.4 Comparison of long-lived radionuclides (^{226}Ra and ^{228}Ra) with ^{224}Ra in LIS

Our data for ^{226}Ra and ^{228}Ra in LIS are not detailed enough to permit mass balances to be constructed for those Ra isotopes. However, samples from the central transect of LIS taken in spring 2009 and summer 2010 show a seasonal difference with higher activities, especially for ^{228}Ra, in summer (Fig. 5). The activities of the parent isotopes ^{230}Th and ^{232}Th, are approximately equal in LIS sediments (Cochran, 1979) and thus the production rate of ^{226}Ra in the muddy sediment of central and western LIS and in the coarse-grained beach sediment characteristic of the Long Island's north shore and the Connecticut coast is slow compared with the other Ra isotopes. Pore water ^{226}Ra concentrations are accordingly low (Cochran 1979, 1985). As a consequence, seasonal changes in ^{226}Ra in the LIS water column are likely to be related to releases of ^{226}Ra associated with manganese oxides in the sediments and thus varying with dissolved manganese.

In contrast, there are significant fluxes of ^{228}Ra from the sediments of LIS, with long-term values of ~35 to 80 dpm m^{-2} d^{-1} based on the ^{228}Ra deficiency in muddy sediment cores from LIS (Cochran, 1979, 1985; Turekian et al. 1996). Although the production rate of ^{228}Ra is also slower than that of ^{224}Ra in the sediments of LIS, the flux of ^{228}Ra is likely to be dependent on the intensity of bioirrigation and the redox cycle of manganese and thus seasonally variable as is that for ^{224}Ra. Moreover, because the ^{228}Ra production rate is significantly lower than that of ^{224}Ra, it also seems likely that its flux from tidal percolation through coarse-grained sediments along shore will be less. Thus a detailed ^{228}Ra mass balance in LIS may permit other terms, such as the flux from sediments and input of fresh SGD to be better determined.

6. Summary

The results presented in this work demonstrate the difficulty in determining SGD fluxes using the short-lived Ra isotopes in an estuary such as Long Island Sound (LIS), in which manganese redox cycling is active due to seasonal development of hypoxia and there is a flux of Ra from bottom sediments, mediated by diffusion and bioirrigation. Based on a spatial survey of ^{224}Ra at ~25 stations in LIS conducted in spring 2009 and summer 2009 and 2010, the water column inventories of ^{224}Ra in LIS are higher in bottom waters than in surface waters and, for the whole water column, are a factor of ~2 greater in the summer than in the spring. These differences are likely due to variation in the flux of ^{224}Ra from bottom sediments as a result of seasonal changes in bioirrigation and/or redox cycling of Mn. Season variation in the rate of resuspension of bottom sediments and desorption of ^{224}Ra from this material also may be a factor.

The ^{224}Ra flux from bottom sediments, measured in oxic core incubation experiments, ranges from 127 – 312 dpm m^{-2} d^{-1} in the muddy sediments of LIS and is ~60 dpm m^{-2} d^{-1} in sandy mud. Imposing hypoxic conditions on the flux cores produces temporally variable fluxes that initially decrease from the oxic value but then increase and can exceed it. Inclusion of the flux of ^{224}Ra from bottom sediments and from desorption from resuspended sediments in a Ra mass balance shows a net input to LIS that we attribute to submarine groundwater discharge. Higher activities of ^{224}Ra in stations taken nearshore and in pore waters of the coarse beach sands along the Long Island and Connecticut shores of LIS (Bokuniewicz et al., submitted) suggest that tidal percolation of water through the beach face is responsible for most of the input of ^{224}Ra from SGD to LIS. Estimates of the magnitude of this flux by Bokuniewicz et al. (submitted) show it to be sufficient to account for the inferred SGD term in the ^{224}Ra balance of LIS.

Our results suggest that processes such as bioirrigation and diffusion in bottom sediments provide an important source of ^{224}Ra to the overlying water column. In estuarine systems that experience seasonal hypoxia, the effects of low dissolved oxygen on the benthic community and on the redox cycling of elements such as Mn can moderate the flux of ^{224}Ra from the sediments. Attributing excesses of ^{224}Ra in the water column in such systems solely to SGD is not justified, and Ra mass balances must take into account other sources, such as bottom sediments, for an accurate estimation of SGD.

7. Acknowledgments

This project has been funded by New York Sea Grant (Project R/CCP-16) and the Ministerio de Ciencia e Innovación (CTM2010-11232-E) and we are grateful for their support. Support from the government of Spain and the Fulbright Commission for a post-doctoral fellowship to J.G-O. (ref 2007-0516) is gratefully acknowledged. Portions of this work comprise the Masters thesis of JWRD. We thank David Bowman and the crews of the R/V *Seawolf* for their assistance in sampling, and Professor Robert Aller for helpful discussions.

8. References

Aller, R.C., 1977. Diagenetic processes near the sediment-water interface of Long Island Sound. II. Fe and Mn. Advances in Geophysics 22, 351–415.

Aller, RC., 1994. The sedimentary Mn cycle in Long Island Sound: Its role as intermediate oxidant and the influence of bioturbation, O_2, and C_{org} flux on diagenetic reaction balances. Journal of Marine Research 52, 259–295.

Anderson, T.H., Taylor, G.T., 2001. Nutrient pulses, plankton blooms, and seasonal hypoxia in western Long Island Sound. Estuaries 24, 228–243.

Beck, A.J., Rapaglia, J.P., Cochran, J.K., Bokuniewicz, H.J., 2007. Radium mass-balance in Jamaica Bay, NY: Evidence for a substantial flux of submarine groundwater. Marine Chemistry 106, 419–441.

Beck, A.J., Rapaglia, J.P., Cochran, J.K., Bokuniewicz, H.J., Yang, S., 2008. Submarine groundwater discharge to Great South Bay, NY, estimated using Ra isotopes. Marine Chemistry 109, 279–291.

Benninger, L.K., 1976. The uranium-series radionuclides as tracers of geochemical processes in Long Island Sound. Ph.D. Dissertation, Yale University. New Heaven, CT.

Blumberg, A.F., Pritchard D.W., 1997. Estimates of the transport through the East River, New York. Journal of Geophysical Research 102, 5685–5703.

Boehm, A.B., Paytan, A., Shellenbarger, G.G., Davis, K.A., 2006. Composition and flux of groundwater from a California beach aquifer: Implications for nutrient supply to the surf zone. Continental Shelf Research 26, 269–282.

Bokuniewicz H., McTiernan, L., Davis, W. 1991. Measurement of sediment resuspension rates in Long Island Sound. Geo-Marine Letters 11, 159-161.

Bollinger, M.S., Moore, W.S., 1984. Radium fluxes from a salt marsh. Nature 309, 444 - 446.

Bollinger, M.S., Moore, W.S., 1993. Evaluation of salt marsh hydrology using radium as a tracer. Geochimica and Cosmochimica Acta 57, 2203–2212.

Burnett, W.C., Bokuniewicz, H., Huettel, M., Moore, W.S., Taniguchi, M., 2003. Groundwater and porewater inputs to the coastal zone. Biogeochemistry 66, 3-33.

Burnett, W.C., Dulaiova, H., 2003. Estimating the dynamics of groundwater input into the coastal zone via continuous radon-222 measurements. Journal of Environmental Radioactivity 69, 21–35.

Cable, J.E., Burnett, W.C., Chanton, J.P., Weatherly, G.L. 1996. Estimating groundwater discharge into the northeastern Gulf of Mexico using radon-222. Earth and Planetary Science Letters 144, 591–604.

Cai, P., Peng, S., Moore, W.S., Shi, X., Wang, G., Dai, M. 2013. ^{224}Ra:^{228}Th disequilibrium in coastal sediments: Implications for solute transfer across the sediment-water interface. Geochemica and Cosmochimica Acta. Accepted Manuscript.

Charette, M.A., Splivallo, R., Herbold, C., Bollinger, M.S., Moore, W.S. 2003. Salt marsh submarine groundwater discharge as traced by radium isotopes. Marine Chemistry 84, 113–121.

Charette M.A., Buesseler, K.O. 2004. Submarine groundwater discharge of nutrients and copper to an urban subestuary of Chesapeake bay (Elizabeth River). Limnology and Oceanography 49, 376–385.

Cochran, JK. 1979. The Geochemistry of ^{226}Ra and ^{228}Ra in Marine Deposits, Ph.D. Thesis, Yale University, New Haven, CT.

Dion, E.P. 1983. Trace elements and radionuclides in the Connecticutt and Amazon river estuary, Ph.D. Thesis, 233 pp., Yale Univ., New Haven, CT.

Garcia-Orellana, J., Cochran, J.K., Bokuniewicz, H., Yang, S., Beck, A.J. 2010. Time-series sampling of ^{223}Ra and ^{224}Ra at the inlet to Great South Bay (New York): a strategy for characterizing the dominant terms in the Ra budget of the bay. Journal of Environmental Radioactivity 101, 582 - 588.

Garcia-Orellana, J., Rodellas, V., Casacuberta, N., López-Castillo, E., Vilarrasa, M., Moreno, V., Garcia-Solsona, E., Masqué, P. 2013. Submarine Groundwater Discharge as a source of natural radioactivity. Marine Chemistry 156, 61-72.

Garcia-Solsona, E., Masqué, P., Garcia-Orellana, J., Rapaglia, J., Beck, A.J., Cochran, J.K., Bokuniewicz, H.J., Zaggia, L., Collavini, F., 2008a. Estimating submarine groundwater discharge around Isola La Cura, northern Venice Lagoon (Italy), by using the radium quartet. Marine Chemistry 109, 292 - 306.

Garcia-Solsona, E., Garcia-Orellana, J., Masqué, P., Dulaiova, H. 2008b. Uncertainties associated with ^{223}Ra and ^{224}Ra measurements in water via a delayed coincidence counter (RaDeCC). Marine Chemistry 109, 198 - 219.

Garcia-Solsona, E., Garcia-Orellana, J., Masque, P., Garces, E., Radakovitch, O., Mayer, A., Estrade, S., Basterretxea, G., 2010. An assessment of karstic submarine groundwa- ter and associated nutrient discharge to a Mediterranean coastal area (Balearic Islands, Spain) using radium isotopes. Biogeochemistry 97 (2–3), 211–229.

Hancock, G.J., Webster, I.T., Ford P.W., Moore, W.S. 2000. Using Ra isotopes to examine transport processes controlling benthic fluxes into a shallow estuarine lagoon. Geochimica and Cosmochimica Acta 64, 3685–3699.

Jensen, L.M., Sand-Jensen, K., Marcher, S., Hansen, M. 1990. Plankton community respiration along a nutrient gradient in a shallow Danish estuary. Marine Ecology Progress Series 61, 75–85.

Kelly, R.P., Moran S.B. 2002. Seasonal changes in groundwater input to a well-mixed estuary estimated using radium isotopes and implications for coastal nutrient budgets. Limnology and Oceanography 47, 1796–1807.

Kim, B.H., and Bokuniewicz, H.J., 1991, Estimates of sediment fluxes in Long Island Sound. Estuaries 14, 237-247.

Krest, J.M., Moore, W.S., Gardner, L.R., Morris, J.T. 2000. Marsh nutrient export supplied by groundwater discharge: Evidence from radium measurements. Global Biogeochemical Cycles 14, 167–76.

Krest J.M., Harvey J.W. 2003. Using natural distributions of short-lived radium isotopes to quantify groundwater discharge and recharge. Limnology and Oceanography 48, 290–8.

Lee, Y.J., Lwiza, K.M.M. 2005. Interannual variability of temperature and salinity in shallow water: Long Island Sound, New York. Journal of Geophysical Research 110, C09022.

Mackin, J., Aller, R., Vigil, H., Rude, P. 1991. Nutrient and dissolved oxygen fluxes across the sediment-water interface. In Long Island Sound Study Final Report, Sediment Geochemistry and Biology, US-EPA Contract CE 002870026. Section IV: 1–252.

Mackin, J.E., Swider, K.T. 1989. Organic matter decomposition pathways and oxygen consumption in coastal marine sediments. Journal of Marine Research 47, 681–716.

McCall, P.L. 1977. Community patterns and adaptive strategies of the infaunal benthos of Long Island Sound. Journal of Marine Research 35, 221-266

Moore, W.S., Arnold R. 1996. Measurement of ^{223}Ra and ^{224}Ra in coastal waters using a delayed coincidence counter. Journal of Geophysical Research 101, 1321–1329.

Moore, W.S. 1997. High fluxes of radium and barium from the mouth of the Ganges-Brahmaputra River during low river discharge suggest a large groundwater source. Earth and Planetary Science Letters 150, 141-150.

Moore, W.S. 2000. Determining coastal mixing rates using radium isotopes. Continental Shelf Research 20, 1993-2007.

Moore, W.S. 2003. Sources and fluxes of submarine groundwater discharge delineated by radium isotopes. Biogeochemistry 66, 75–93.

Moore, W.S. 2010. The Effect of Submarine Groundwater Discharge on the Ocean. Annual Review of Marine Science 2, 59–88.

Moore, W.S., Sarmiento, J.L., Key, R.M. 2008. Submarine groundwater discharge revealed by ^{228}Ra distribution in the upper Atlantic Ocean. Nature Geosciences 1, 309–11.

Parker, C.A., O'Reilly, J.E. 1991. Oxygen depletion in Long Island Sound: a historical perspective. Estuaries 14, 248–264.

Pluhowski, E.J., Kantrowitz, I.H. Hydrology of the Babylon–Islip Area, Suffolk County, Long Island, New York. 1964. US Geological Survey Water Supply Paper 1768, 128 pp.

Robinson, C., Li L., Barry, D.A. 2007. Effect of tidal forcing on a subterranean estuary. Advances in Water Resources. 30, 851- 865.

Rodellas, V., Garcia-Orellana, J., Garcia-Solsona, E., Masqué, P., Domínguez, J.A., Ballesteros, B.J., Mejías, M., Zarroca, M., 2012. Quantifying groundwater discharge from different sources into a Mediterranean wetland by using ^{222}Rn and Ra isotopes. Journal of Hydrology 466–467, 11–22.

Torgersen, T., Turekian, K.K., Turekian, V.C., Tanaka, N., DeAngelo, E., O'Donnell, J. 1996. ^{224}Ra distribution in surface and deep water of Long Island Sound: sources and horizontal transport rates. Continental Shelf Research 16, 1545–1559.

Turner, I.L., Coates, B.P., Acworth R.I. 1997. Tides, waves, and the super-elevation of groundwater at the coast. Journal of Coastal Research 13, 46-60.

Urish, D.W., McKenna, T.E. 2004. Tidal effects on ground water discharge through a sandy marine beach. Ground Water – Oceans 42, 971–982.

Vieira, M.E.C. 1990. Observations of Currents, Temperature and Salinity in Long Island Sound, 1988. A Data Report. Special Data Report #6, Marine Sciences Research Center, State University of New York. Stony Brook, New York, USA.

Vieira, M.E.C. 2000. The long-term residual circulation in Long Island Sound. Estuaries 23, 199–207.

Windom, H.L., Moore, W.S., Niencheski, L.F.H., Jahnke, R.A. 2006. Submarine groundwater discharge: a large, previously unrecognized source of dissolved iron to the South Atlantic Ocean. Marine Chemistry 102, 252–266.

<u>TABLES</u>

Table 1. Mean ^{224}Ra concentrations in the different basins of Long Island Sound in spring 2009 and summer 2009 and 2010.

Table 2. ^{224}Ra fluxes from LIS sediment cores incubated under oxic, well-mixed conditions and hypoxic conditions.

Table 3. ^{224}Ra inventories in western, central and eastern LIS in spring 2009 and summer 2010.

Table 4. ^{224}Ra mass balance in Long Island Sound.

Supplemental Data - Tables

Table S1. Location and physico-chemical data (T^a, S, DO, SPM, Mn_{aq}, Mn_s) for LIS campaigns.

Table S2. Ra activities for LIS sampling campaigns in 2009 and 2010.

Table S3. Water and organic content and solid phase manganese concentrations in LIS sediment cores

Table S4. Solid phase U/Th series activities from incubation cores sampled after completion of the incubation experiments.

Table S5. Pore water ^{224}Ra and ^{223}Ra from incubation cores sampled after completion of the incubation experiments.

FIGURES

Figure 1: (a) Map of Long Island Sound showing sub-basins and major geographic features, (b) Sampling stations in Long Island Sound. Stations were oriented along 4 transects: one axial from the Narrows to the Race and three cross-Sound transects in the delimited western, central and eastern Sound.

Figure 2. Temperature, salinity and DO profiles in stations along the axial transects in spring (2009) and summer (2010).

Figure 3. ^{224}Ra concentrations in surface and deep waters in the campaigns carried out in April 2009, July 2010 and August 2010.

Figure 4. Surface and deep ^{224}Ra during spring 2009 and summer 2010 concentrations along the three longitudinal transects.

Figure 5. $^{228,226}Ra$ activities in samples collected along the central transect of Long Island Sound in 2009 and 2010.

Figure 6. Dissolved (Mn_{aq}) and particulate Mn (Mn_p) from surface and deep LIS samples.

Figure 7. ^{224}Ra fluxes ($dpm \cdot m^{-2}$) over time for sediment cores collected in 2010 and incubated initially in an oxic mode then allowed to become hypoxic.

Figure 8. Mn(aq) fluxes and accompanying DO concentrations over time for summer oxic Mn flux cores for ST8 (a) and ST16 (b) and for summer anoxic to anoxic winter oxic Mn flux for ST8 (c) and ST16 (d). Core temperatures for summer and winter phases were 21ºC and 2.5ºC, respectively.

Figure 9. a) LIS Summer 2010 surface and deep Mn(aq) concentrations plotted against corresponding DO concentrations. b) LIS summer 2010 surface and deep ^{224}Ra concentrations plotted against corresponding DO concentrations. A correlation between deep Mn(aq) - ^{224}Ra and DO values is observed.

Supplemental Figures

Figure S1. Correlation between ^{224}Ra and ^{223}Ra showing an identical distribution of both radionuclides in LIS.

Figure S2. ^{224}Ra accumulated in the overlying water of oxic incubation cores vs. time. Slope of the best-fit lines gives the ^{224}Ra flux in dpm m^{-2} d^{-1}.

Figure S3. Radiographs of ST8 (a) and ST16 (b) subcores collected in Summer 2010.

Table 1.

Spring 2009	Surface	Deep
	(dpm·100L^{-1})	
Western Basin	3.40 ± 1.57	6.94 ± 1.35
Central Basin	4.56 ± 1.89	5.72 ± 2.02
Eastern Basin	6.26 ± 1.29	5.63 ± 1.03
Mean	**4.7 ± 1.4**	**6.1 ± 0.7**
Summer 2009		
Western Basin	12.65 ± 5.54	15.51 ± 3.82
Central Basin	7.29 ± 3.06	12.71 ± 3.30
Eastern Basin	7.34 ± 1.60	7.25 ± 0.87
Mean	**9.1 ± 3.1**	**11.8 ± 4.2**
Summer 2010		
Western Basin	11.91 ± 5.94	18.20 ± 4.50
Central Basin	7.39 ± 5.48	16.59 ± 6.60
Eastern Basin	6.14 ± 3.74	8.22 ± 2.81
Mean	**8.5 ± 3.0**	**14.3 ± 5.4**

Table 2.

Sediment	Core	^{224}Ra flux ($dpm \cdot m^{-2} \cdot d^{-1}$)	
		Oxic incubations	Hypoxic incubations**
Muddy	ST 16	127 ± 12*	75 → 214 → 170
	ST 13	313 ± 16	n.d.
	ST 120E	170 ± 7	n.d.
	ST 8	164 ± 13*	50 → 140 → 70
Sandy	STWM	57 ± 3	n.d.

n.d.: not determined

*Mean ± 1SD of individual fluxes over course of oxic incubation (see Fig. 7)

**Values indicate variation in flux with time (~7 days) after start of hypoxic incubation (see Fig. 7)

Table 3.

	Basin	Water Volume (L)	Spring 2009		Summer 2010	
			Mean ^{224}Ra concentration ($dpm \cdot 100L^{-1}$)	^{224}Ra Inventory (dpm)	Mean ^{224}Ra concentration ($dpm \cdot 100L^{-1}$)	^{224}Ra Inventory (dpm)
Surface	Eastern basin	$3.40 \cdot 10^{12}$	6.08 ± 1.40	$(2.07 \pm 0.48) \cdot 10^{11}$	6.53 ± 4.04	$(2.22 \pm 1.37) \cdot 10^{11}$
	Central basin	$2.90 \cdot 10^{12}$	4.92 ± 1.37	$(1.43 \pm 0.40) \cdot 10^{11}$	7.50 ± 6.26	$(2.17 \pm 1.82) \cdot 10^{11}$
	Western basin	$1.87 \cdot 10^{12}$	4.73 ± 1.76	$(0.88 \pm 0.33) \cdot 10^{11}$	11.91 ± 5.94	$(2.23 \pm 1.11) \cdot 10^{11}$
Deep	Eastern basin	$1.88 \cdot 10^{13}$	5.10 ± 1.33	$(9.58 \pm 2.51) \cdot 10^{11}$	8.40 ± 3.10	$(15.80 \pm 5.82) \cdot 10^{11}$
	Central basin	$1.76 \cdot 10^{13}$	5.70 ± 2.26	$(10.02 \pm 3.98) \cdot 10^{11}$	15.68 ± 5.85	$(27.59 \pm 10.29) \cdot 10^{11}$
	Western basin	$7.42 \cdot 10^{12}$	6.92 ± 1.26	$(5.14 \pm 0.94) \cdot 10^{11}$	18.20 ± 4.50	$(13.50 \pm 3.34) \cdot 10^{11}$
Total		$5.20 \cdot 10^{13}$		$(29.1 \pm 4.8) \cdot 10^{11}$		$(63.5 \pm 12.5) \cdot 10^{11}$

Considered stations for: Eastern basin (1, 2, 3, 4, 101, 102)
Central basin (113E, 113W, 5, 6, 7, 8, 9, 117)
Western basin (10, 120E, 120W, 11, 12, 13, 14, 15, 16, 17, 18)

Table 4.

	^{224}Ra ($\cdot 10^{12}$ dpm$\cdot$y^{-1})	
	SPRING 2009	SUMMER 2010
Fluxes OUT		
LIS to Block Island Sound	34.2 ± 8.0	41.6 ± 16.0
LIS to East river/NY Harbor	4.4 ± 1.0	11.6 ± 2.9
Decay	205 ± 34	447 ± 88
Fluxes IN		
Block Island Sound to LIS	21.3 ± 1.4	21.3 ± 1.4
East River to LIS	4.1 ± 0.9	4.1 ± 0.9
Connecticut River	1.4 ± 0.1	2.0 ± 0.4
Desorption during resuspension	31 ± 27	82 ± 51
Diffusion and bioirrigation from sediments	80 ± 24	147 ± 44
SGD	**106 ± 50**	**244 ± 112**
SGD from shoreline flux	**173**	

Figure 1

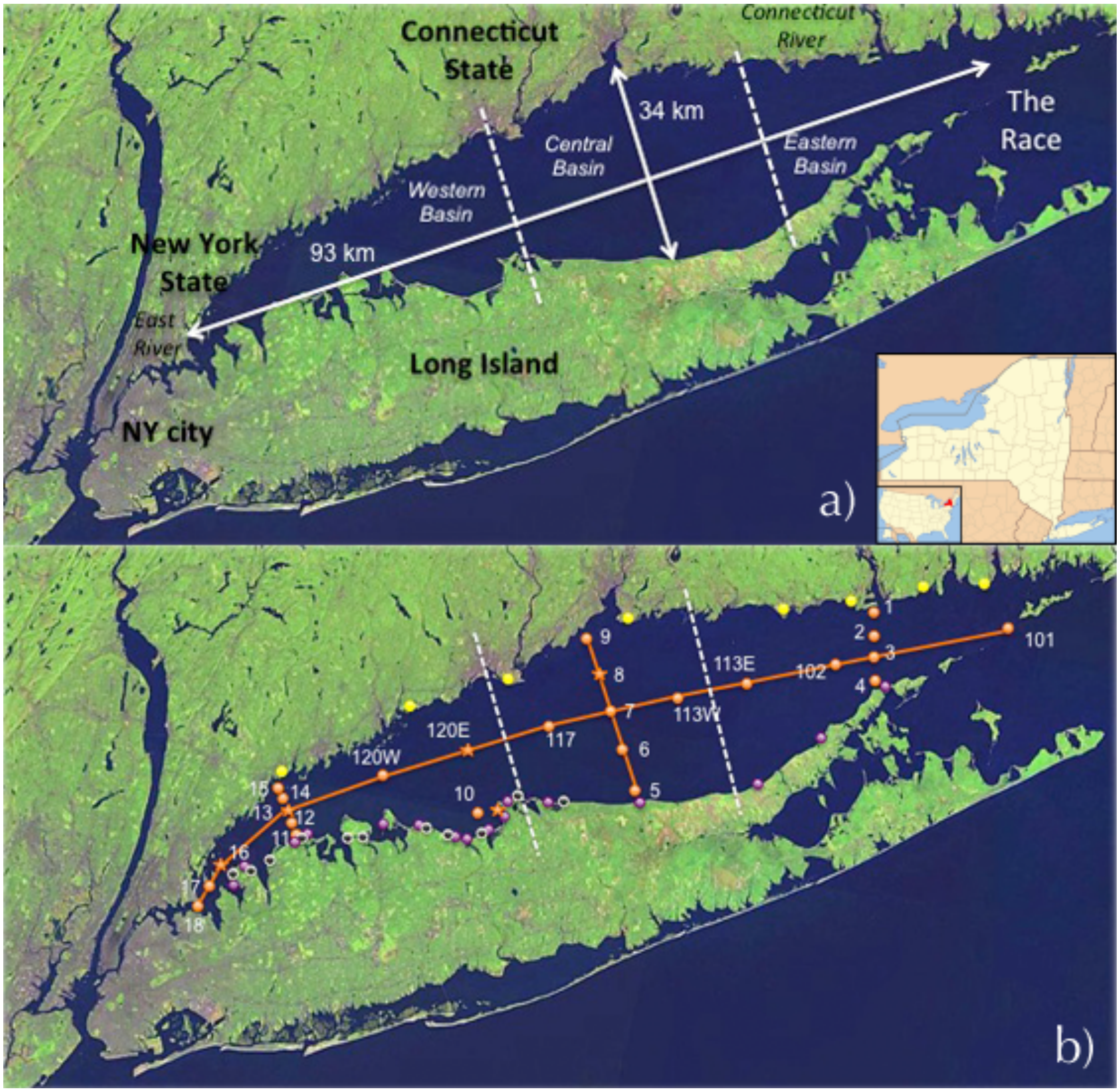
Connecticut State
Connecticut River
34 km
The Race
Central Basin
Western Basin
Eastern Basin
New York State
93 km
East River
Long Island
NY city
a)
1
2
3
4
5
6
7
8
9
10
11
12
13
14
15
16
17
18
101
102
113E
113W
117
120E
120W
b)

Figure 2

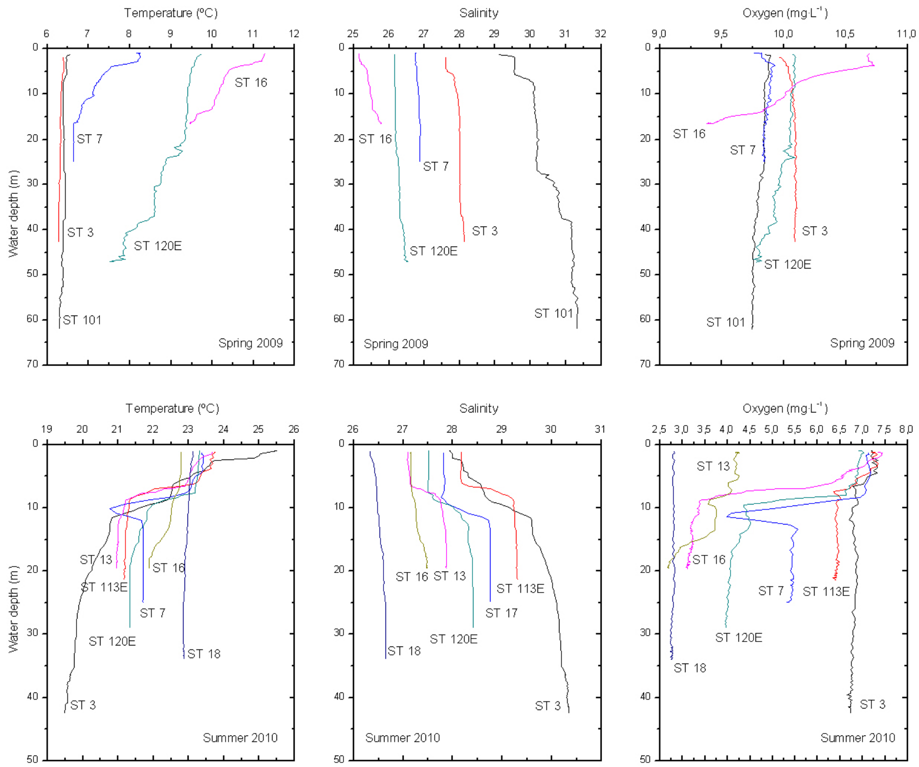
Temperature (ºC)
Salinity
Oxygen (mg L⁻¹)
Water depth (m)
ST 16
ST 7
ST 3
ST 120E
ST 101
Spring 2009
ST 13
ST 113E
ST 17
ST 18
Summer 2010

Figure 3

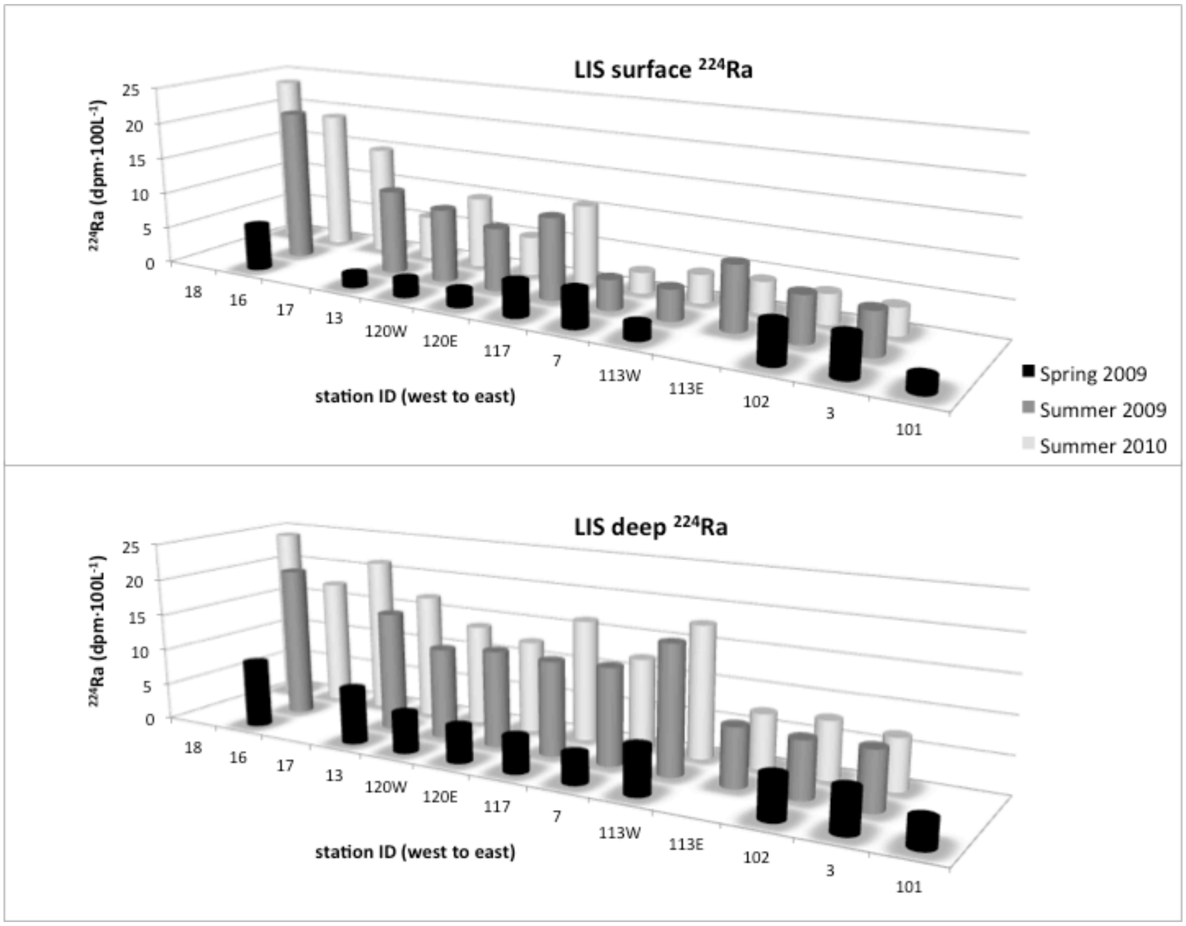
LIS surface ²²⁴Ra
²²⁴Ra (dpm·100L⁻¹)
25
20
15
10
5
0
18
16
17
13
120W
120E
117
7
113W
113E
102
3
101
station ID (west to east)
Spring 2009
Summer 2009
Summer 2010
LIS deep ²²⁴Ra
²²⁴Ra (dpm·100L⁻¹)
25
20
15
10
5
0
18
16
17
13
120W
120E
117
7
113W
113E
102
3
101
station ID (west to east)

Figure 4

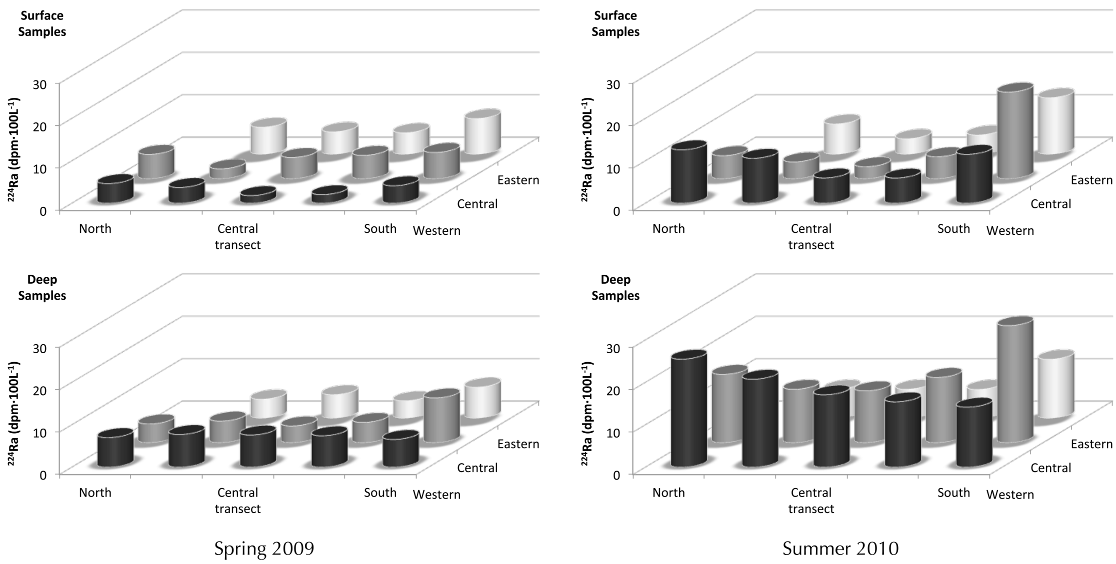
Surface Samples
Deep Samples
224Ra (dpm·100L-1)
0
10
20
30
North
Central transect
South
Western
Central
Eastern
Spring 2009
Summer 2010

Figure 5

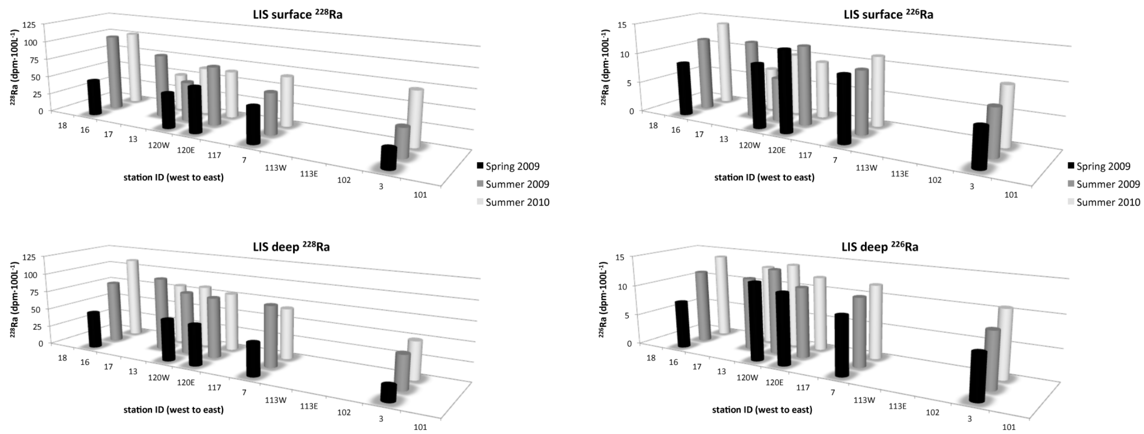
LIS surface ²²⁸Ra
²²⁸Ra (dpm·100L⁻¹)
125
100
75
50
25
0
18
16
17
13
120W
120E
117
7
113W
113E
102
3
101
station ID (west to east)
Spring 2009
Summer 2009
Summer 2010
LIS surface ²²⁶Ra
²²⁶Ra (dpm·100L⁻¹)
15
10
5
0
station ID (west to east)
Spring 2009
Summer 2009
Summer 2010
LIS deep ²²⁸Ra
²²⁸Ra (dpm·100L⁻¹)
station ID (west to east)
LIS deep ²²⁶Ra
²²⁶Ra (dpm·100L⁻¹)
station ID (west to east)

Figure 6

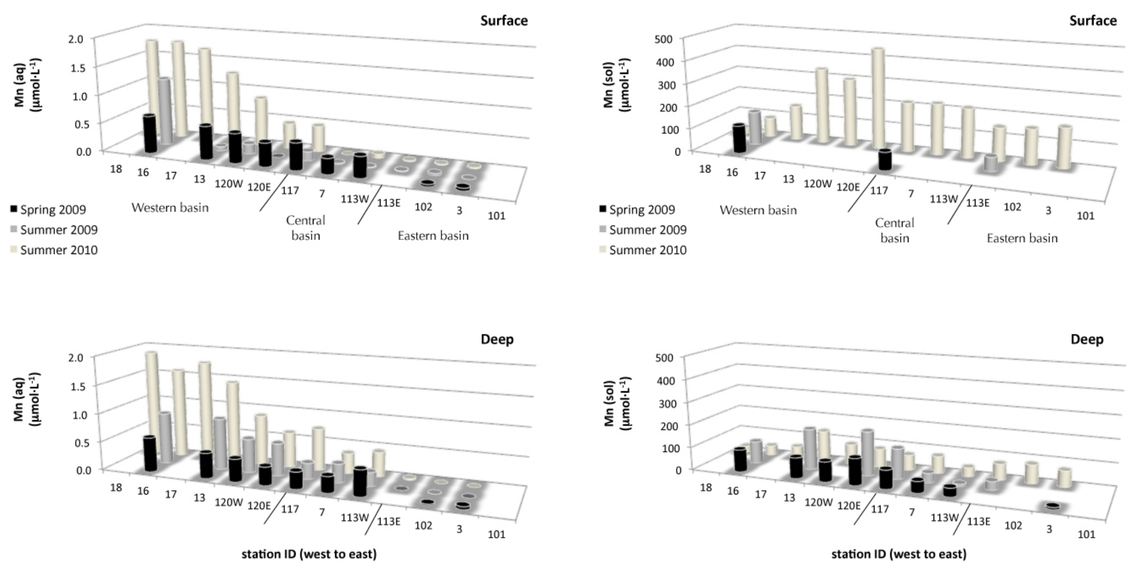

Surface
Deep
Mn (aq) (µmol·L⁻¹)
Mn (sol) (µmol·L⁻¹)
2.0
1.5
1.0
0.5
0.0
500
400
300
200
100
0
18
16
17
13
120W
120E
117
7
113W
113E
102
3
101
Spring 2009
Summer 2009
Summer 2010
Western basin
Central basin
Eastern basin
station ID (west to east)

Figure 7

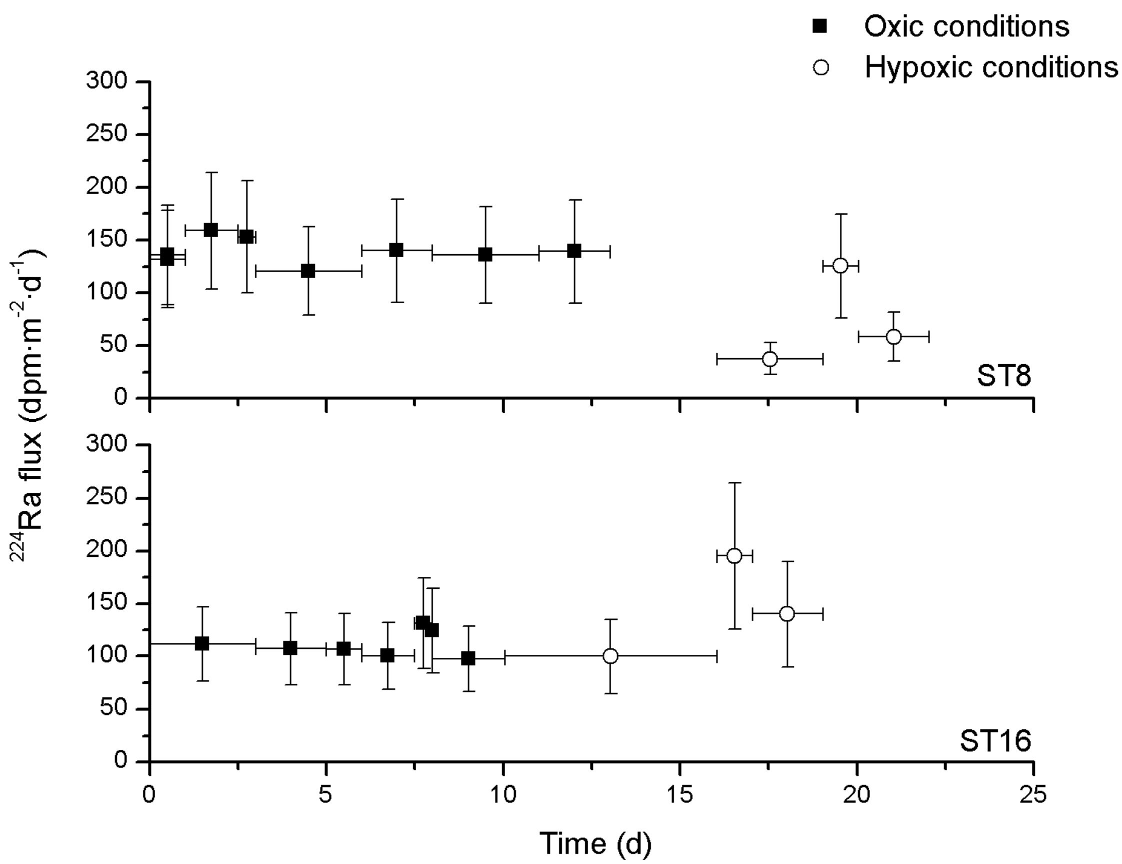
Oxic conditions
Hypoxic conditions
ST8
ST16
224Ra flux (dpm·m-2·d-1)
Time (d)
0
5
10
15
20
25
0
50
100
150
200
250
300

987 Figure 8

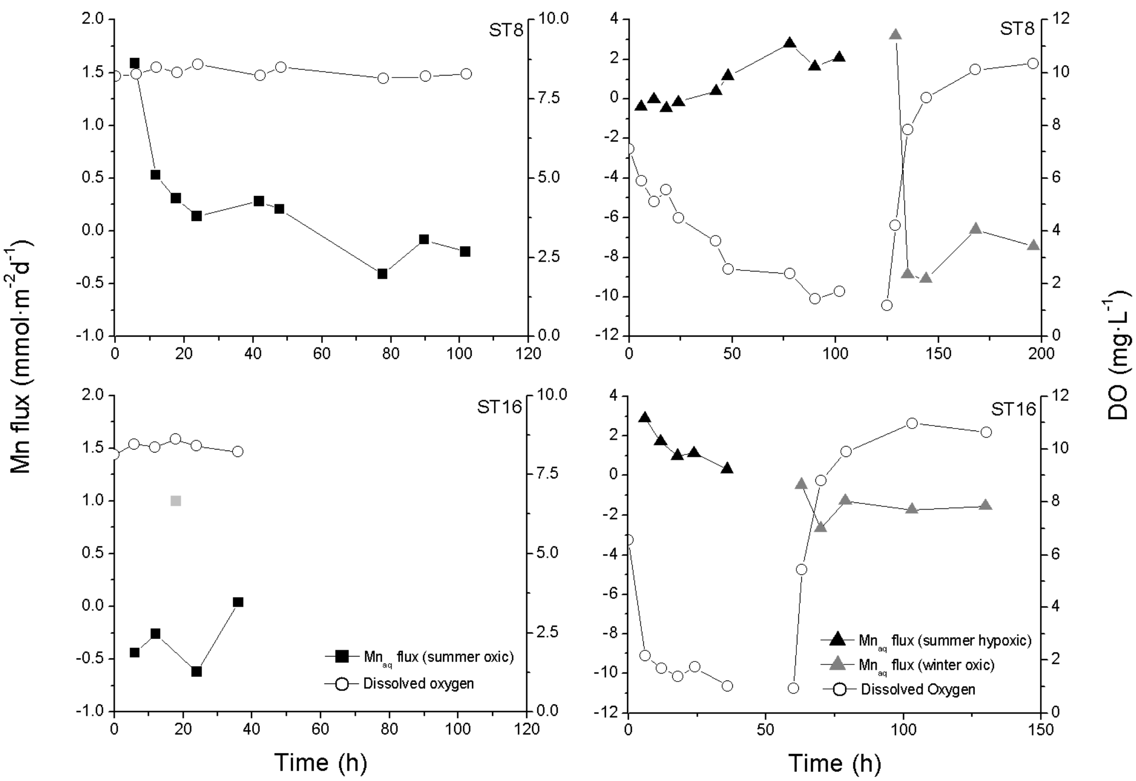

988

Figure 9

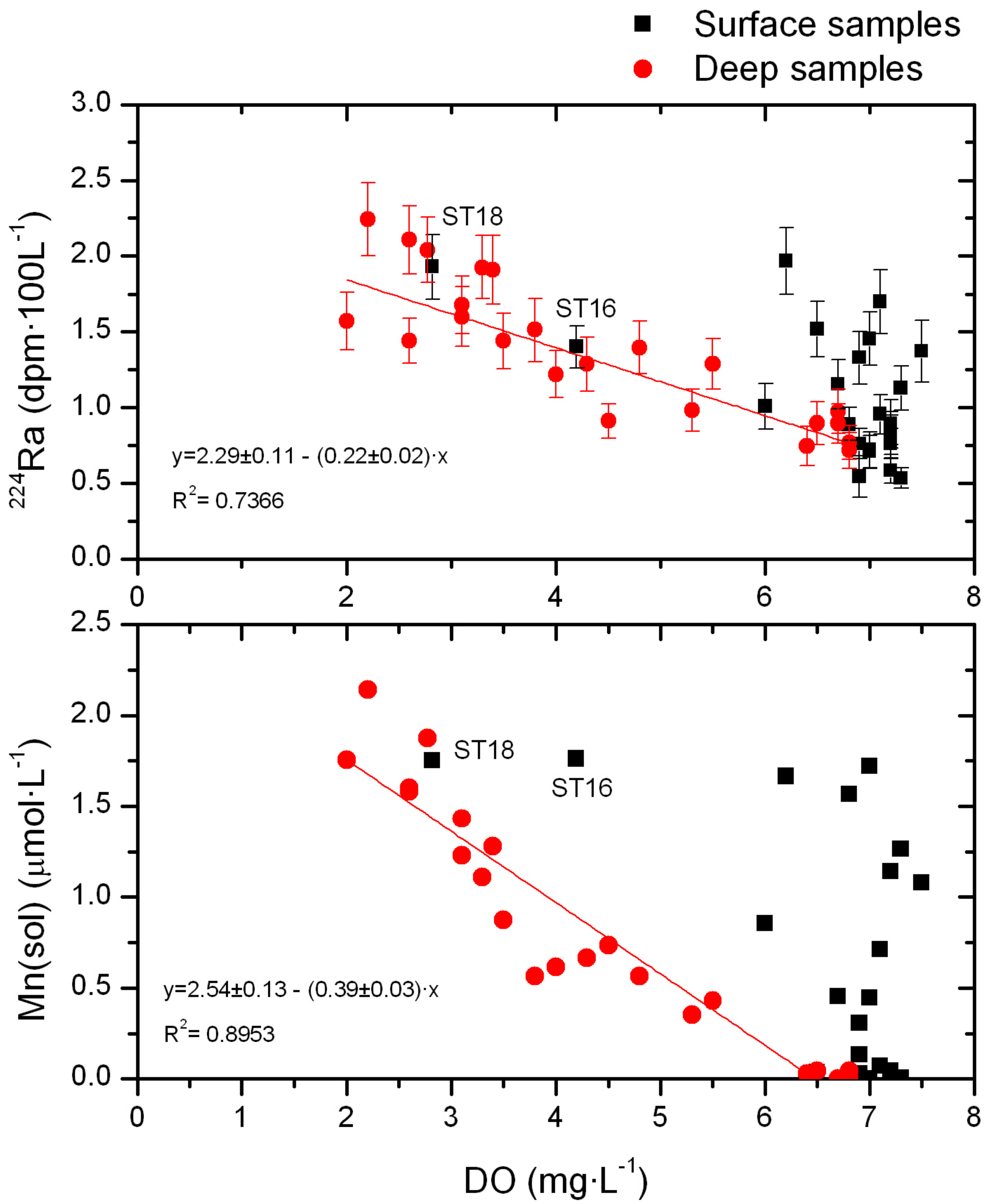
Surface samples
Deep samples
^{224}Ra (dpm·100L^{-1})
ST18
ST16
y=2.29±0.11 - (0.22±0.02)·x
R^2= 0.7366
Mn(sol) (μmol·L^{-1})
ST18
ST16
y=2.54±0.13 - (0.39±0.03)·x
R^2= 0.8953
DO (mg·L^{-1})

Figure S1

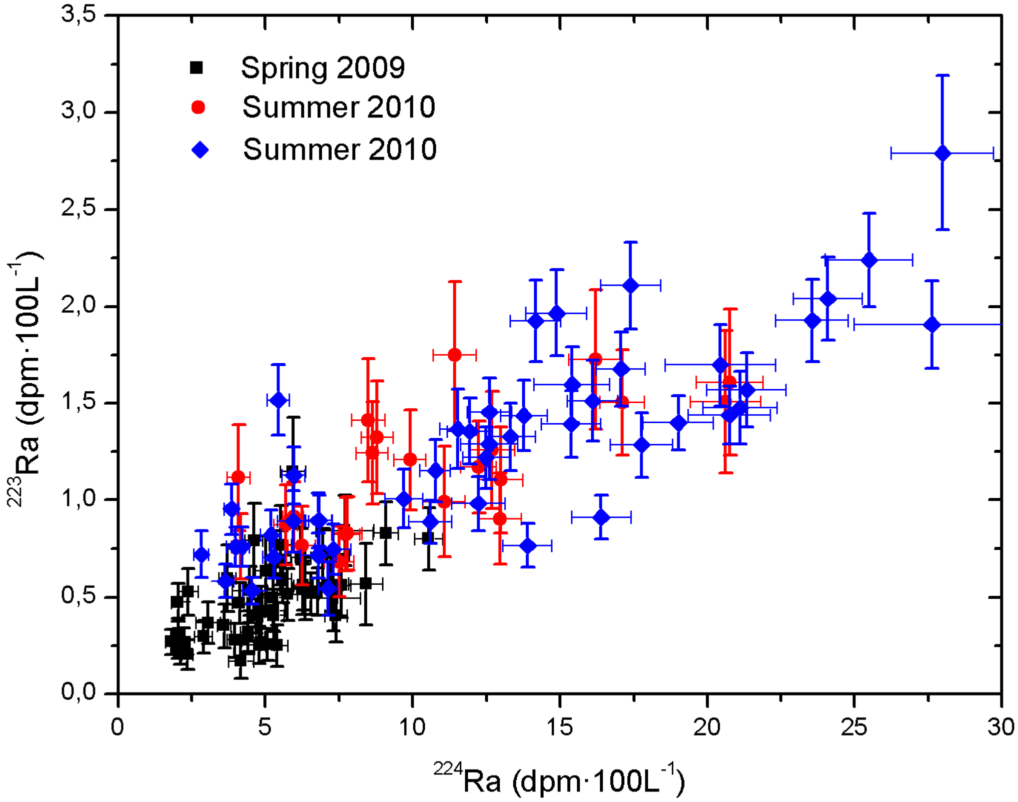
Spring 2009
Summer 2010
Summer 2010
3,5
3,0
2,5
2,0
1,5
1,0
0,5
0,0
0
5
10
15
20
25
30
223Ra (dpm·100L-1)
224Ra (dpm·100L-1)

994 Figure S2

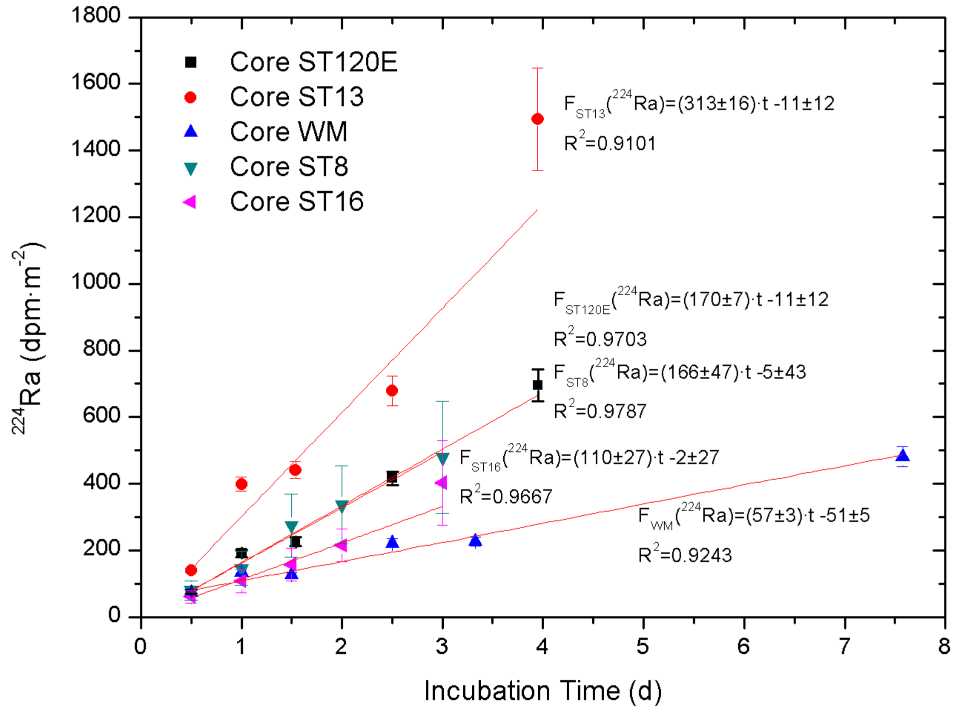

995

Figure S3

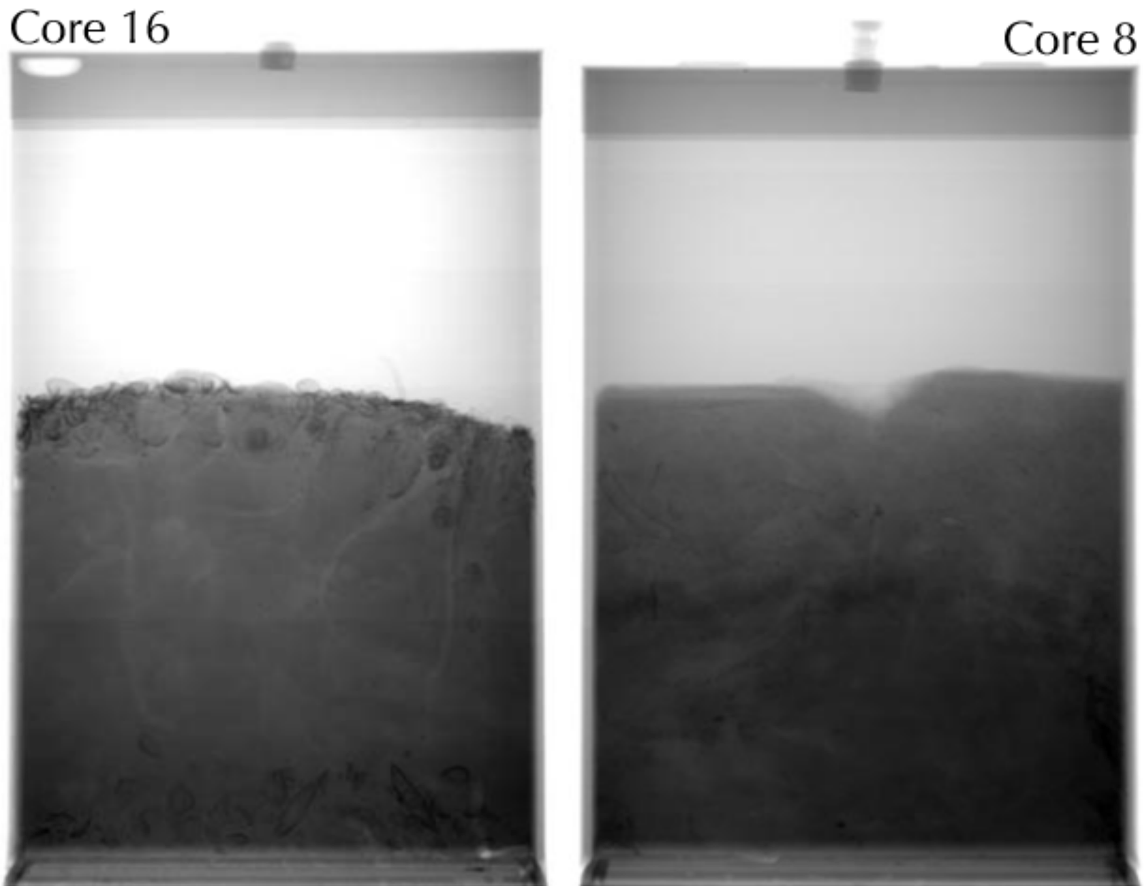

Supplemental Data - Table S1. T^a, S, DO, SPM, Mn_{aq}, Mn_s

SPRING 2009	Sampling hour	Coordinates		Depth	Sampling depth	Salinity	T^a	DO	SPM	Mn_{aq}	Mn_p
		Latitude (N)	Longitude (W)	(m)	(m)		(ºC)	$mg \cdot L^{-1}$	$mg \cdot L^{-1}$	$\mu mol \cdot L^{-1}$	$\mu mol \cdot g^{-1}$
$ST1_{surf}$	24/04/09 04:35	41° 15.02’	72° 20.03’	9	0.5	20.8	6.8	10.1	4.73		
$ST1_{deep}$	24/04/09 04:25	41° 15.02’	72° 20.03’	9	8	27.3	6.3	10	8.50		
$ST2_{surf}$	24/04/09 05:30	41° 13.17’	72° 19.56’	41	0.5	27.7	9.9	9.9	0.86		
$ST2_{deep}$	24/04/09 05:30	41° 13.17’	72° 19.56’	41	40	29	7.7	9.9	0.74		
$ST3_{surf}$	24/04/09 06:15	41° 11.51’	72° 20.01’	43	0.5	27.6	7.6	9.9	0.33	0.05	627
$ST3_{deep}$	24/04/09 06:15	41° 11.51’	72° 20.01’	43	42	28.1	7.5	10	2.55	0.05	9
$ST4_{surf}$	24/04/09 06:50	41° 09.532’	72° 20.080’	25	0.5	27.4	7.7	10.1	1.09		
$ST4_{deep}$	24/04/09 06:50	41° 09.532’	72° 20.080’	25	22	27.9	7.7	10.1	2.13		
$ST101_{surf}$	24/04/09 09:00	41° 14.209’	72° 03.594’	70	0.5	29.1	8.1	10.1	0.98		
$ST101_{deep}$	24/04/09 09:00	41° 14.209’	72° 03.594’	70	61	31.3	7.2	9.9	1.56		
$ST102_{surf}$	24/04/09 11:50	41° 09.848’	72° 25.740’	49	0.5	28.1	9.4	9.7	0.51	0.04	74
$ST102_{deep}$	24/04/09 11:50	41° 09.848’	72° 25.740’	49	46	28.6	7.7	9.9	0.40	0.02	323
$ST5_{surf}$	28/04/09 08:50	40° 59.018’	72° 52.028’	21	0.5	26.5	10.5	10	1.03		
$ST5_{deep}$	28/04/09 08:50	40° 59.018’	72° 52.028’	21	18	26.5	9.5	10	1.11		
$ST6_{surf}$	28/04/09 09:30	41° 02.329’	72° 53.610’	37	0.5	26.5	10.9	10	0.78		
$ST6_{deep}$	28/04/09 09:30	41° 02.329’	72° 53.610’	37	35	26.9	7.9	9.9	1.51		
$ST117_{surf}$	28/04/09 10:40	41° 04.993’	73° 03.270’	26	0.5	26.3	11.3	9.9	1.06	0.47	79
$ST117_{deep}$	28/04/09 10:40	41° 04.993’	73° 03.270’	26	23	26.8	8.2	9.8	1.04	0.30	82
$ST7_{surf}$	28/04/09 11:30	41° 05.826’	72° 55.303’	28	0.5	26.7	10.8	9.8	0.84	0.27	73
$ST7_{5m}$	28/04/09 12:45	41° 05.826’	72° 55.303’	28	5	26.8	8.8	9.8	0.66		
$ST7_{15m}$	28/04/09 12:05	41° 05.826’	72° 55.303’	28	14.5	26.9	9.4	9.9	0.97		
$ST7_{deep}$	28/04/09 11:30	41° 05.826’	72° 55.303’	28	25	26.9	8.6	9.9	1.10	0.28	50

ST8$_{surf}$	28/04/09 15:05	41° 09.166’	72° 56.800’	20.5	0.5	26.7	12.1	10	0.68		
ST8$_{deep}$	28/04/09 15:25	41° 09.166’	72° 56.800’	20.5	17	26.7	8.9	10	1.58		
ST113$_{surf}$	28/04/09 13:45	41° 07.329’	72° 45.422’	32	0.5	26.8	12.1	10	0.49	0.37	373
ST113$_{deep}$	28/04/09 13:45	41° 07.329’	72° 45.422’	32	29	26.9	8.9	9.9	2.30	0.45	37
ST9$_{surf}$	28/04/09 16:00	41° 12.446’	72° 58.714’	12	0.5	26.2	13.5	10.4	0.88		
ST9$_{deep}$	28/04/09 16:20	41° 12.446’	72° 58.714’	12	9	26.2	11.3	10.3	1.56		
ST11$_{surf}$	30/04/09 10:25	40° 55.529’	73° 34.271’	15	0.5	25.5	12.0	11.2	1.09		
ST11$_{deep}$	30/04/09 10:25	40° 55.529’	73° 34.271’	15	12.5	26	9.9	9.2	3.15		
ST13$_{surf}$	30/04/09 10:50	40° 57.469’	73° 35.187’	16	0.5	25.6	12.2	11.4	0.93	0.59	149
ST13$_{deep}$	30/04/09 11:00	40° 57.469’	73° 35.187’	16	15	26.2	9.1	9.4	2.32	0.44	91
ST15$_{surf}$	30/04/09 11:25	40° 58.904’	73° 36.499’	13.5	0.5	26	11.5	10.2	0.96		
ST15$_{deep}$	30/04/09 11:25	40° 58.904’	73° 36.499’	13.5	10	26.1	10.0	9.9	1.23		
ST12$_{surf}$	30/04/09 13:50	40° 56.512’	73° 34.614’	0.5	0.5	25.6	13.07	11.2	1.02		
ST12$_{deep}$	30/04/09 13:50	40° 56.512’	73° 34.614’	17	15.5	26.1	10.16	9.2	2.22		
ST14$_{surf}$	30/04/09 14:20	40° 58.364’	73° 35.762’	0.5	0.5	25.9	26.35	10.5	1.33		
ST14$_{deep}$	30/04/09 14:20	40° 58.364’	73° 35.762’	18	15.8	26.3	26.7	9.5	1.68		
ST10$_{surf}$	30/04/09 08:15	40° 56.275’	73° 11.576’	16	0.5	26.2	10.7	10	0.88		
ST10$_{deep}$	30/04/09 08:15	40° 56.275’	73° 11.576’	16	14.2	26.3	9.6	9.6	1.73		
ST120W$_{surf}$	30/04/09 15:30	40° 59.680’	73° 25.231’	52	0.5	26.3	11.0	10	0.72	0.52	168
ST120W$_{deep}$	30/04/09 15:30	40° 59.680’	73° 25.231’	52	47	26.5	8.9	9.7	1.82	0.40	87
ST120E$_{surf}$	30/04/09 16:45	41° 01.975’	73° 13.515’	32	0.5	26.4	11.5	10	0.66	0.41	122
ST120E$_{deep}$	30/04/09 16:45	41° 01.975’	73° 13.515’	32	28	26.7	8.3	9.7	1.21	0.32	117
ST16$_{surf}$	30/04/09 12:35	40° 52.500’	73° 44.944’	18	0.5	25.2	12.4	10.7	1.53	0.66	122
ST16$_{deep}$	30/04/09 12:35	40° 52.500’	73° 44.944’	18	16.4	25.8	10.6	9.4	2.00	0.61	98

Supplemental Data - Table S1. T^{a}, S, DO, SPM, Mn$_{aq}$, Mn$_{s}$ (continuation).

SUMMER 2009	Sampling hour	Coordinates		Depth	Sampling depth	Salinity	T^a	DO	SPM	Mn_{aq}	Mn_{sol}
		Latitude (N)	Longitude (W)	(m)	(m)		(ºC)	$mg \cdot L^{-1}$	$mg \cdot L^{-1}$	$\mu mol \cdot L^{-1}$	$\mu mol \cdot g^{-1}$
$ST16_{surf}$	29/07/09 14:50	40° 52.463'	73° 44.969'	20	0.5	24.9		6.9	2.64	1.19	148
$ST16_{deep}$	29/07/09 14:50	40° 52.463'	73° 44.969'	20	19	25.8		3.8	3.68	0.91	99
$ST13_{surf}$	29/07/09 16:00	40° 57.439'	73° 35.365'	21	0.5	25.7		8.4	1.42	0.07	417
$ST13_{deep}$	29/07/09 16:00	40° 57.439'	73° 35.365'	21	20	26.1		4.2	4.22	0.90	180
$ST120W_{surf}$	29/07/09 12:50	40° 59.699'	73° 25.201'	46	0.5	25.5		9.4	2	0.17	357
$ST120W_{deep}$	29/07/09 12:50	40° 59.699'	73° 25.201'	46	45	26.5		4.2	3.42	0.59	802
$ST120E_{surf}$	29/07/09 10:30	41° 01.960'	73° 13.500'	28	0.5	25.5		8	0.84	0.00	325
$ST120E_{deep}$	29/07/09 10:30	41° 01.960'	73° 13.500'	28	27	26.8		4.6	3.04	0.57	194
$ST117_{surf}$	29/07/09 08:30	40° 04.994'	73° 03.253'	28	0.5	24.9		6.9	0.76	0.16	494
$ST117_{deep}$	29/07/09 09:15	40° 04.994'	73° 03.253'	28	26.7	27		3.5	3.84	0.28	133
$ST7_{surf}$	04/08/09 19:20	41° 05.925'	72° 55.454'	26	0.5	25.4		7	1.24	0.02	195
$ST7_{deep}$	04/08/09 19:20	41° 05.925'	72° 55.454'	26	25	27.2		4.1	5.58	0.33	42
$ST113W_{surf}$	04/08/09 09:50	41° 07.363'	72° 45.583'	29	0.5	25.8		7.5	1.04	0.02	895
$ST113W_{deep}$	04/08/09 09:50	41° 07.363'	72° 45.583'	29	28	27.5		4.7	6.8	0.24	10
$ST113E_{surf}$	04/08/09 11:00	41° 08.653'	72° 35.206'	23	0.5	25.3		8.3	2.22	0.01	61
$ST113E_{deep}$	04/08/09 11:00	41° 08.653'	72° 35.206'	23	22	27.8		5.7	2.22	0.00	37
$ST102_{surf}$	04/08/09 12:00	41° 10.139'	72° 27.721'	28	0.5	27		6.4	1.1	0.04	
$ST102_{deep}$	04/08/09 12:00	41° 10.139'	72° 27.721'	28	27	28.9		5.4	1.14	0.00	
$ST3_{surf}$	04/08/09 11:40	41° 11.556'	72° 19.919'	36	0.5	26.5		7	1.36	0.00	43
$ST3_{deep}$	04/08/09 11:40	41° 11.556'	72° 19.919'	36	35	29.6		5.4	1.1	0.00	60
$ST1_{surf}$	04/08/09 14:15	41° 14.948'	72° 19.928'	92	0.5	29		6.4	1.42		
$ST1_{deep}$	04/08/09 14:15	41° 14.948'	72° 19.928'	92	90	31.1		5.7	0.8		

Supplemental Data - Table S1. T^a, S, DO, SPM, Mn_{aq}, Mn_s (continuation).

SUMMER 2010	Sampling hour	Coordinates		Depth	Sampling depth	Salinity	T^a	DO	SPM	Mn_{aq}	Mn_{sol}
		Latitude (N)	Longitude (W)	(m)	(m)		(ºC)	$mg \cdot L^{-1}$	$mg \cdot L^{-1}$	$\mu mol \cdot L^{-1}$	$\mu mol \cdot g^{-1}$
$ST5_{surf}$	03/08/10 09:45	40° 59.055'	72° 51.867'	21	0.5	27.6	23.0	6.5	1.53		
$ST5_{deep}$	03/08/10 09:45	40° 59.055'	72° 51.867'	21	20	28	21.8	3.8	3.64		
$ST6_{surf}$	03/08/10 10:30	40° 02.299	72° 53.650'	36	0.5	27.6	23.4	6.9	1.19		
$ST6_{deep}$	03/08/10 10:30	40° 02.299	72° 53.650'	36	35	28.6	20.8	4.3	2.63		
$ST117_{surf}$	03/08/10 11:40	40° 04.994'	73° 03.253'	24	0.5	27.7	23.2	6.7	2.31	0.47	79
$ST117_{deep}$	03/08/10 11:40	40° 04.994'	73° 03.253'	24	23	28.6	21.5	4.5	3.79	0.30	82
$ST7_{surf}$	03/08/10 12:35	41° 05.925'	72° 55.454'	26	0.5	27.8	24.0	7	1.05	0.27	73
$ST7_{deep}$	03/08/10 12:35	41° 05.925'	72° 55.454'	26	25	28.8	22.0	5.3	3.36	0.28	50
$ST113W_{surf}$	03/08/10 13:40	41° 07.363'	72° 45.583'	29	0.5	27.7	24.5	7.1	1.10	0.37	373
$ST113W_{deep}$	03/08/10 13:40	41° 07.363'	72° 45.583'	29	28	28.8	22.4	5.5	6.75	0.45	37
$ST8_{surf}$	03/08/10 14:55	41° 09.136'	72° 56.808'	19	0.5	27.8	24.3	7.2	1.50		
$ST8_{deep}$	03/08/10 14:55	41° 09.136'	72° 56.808'	19	18	28.6	22.2	4.8	3.64		
$ST9_{surf}$	03/08/10 15:30	41° 12.434'	72° 58.669'	11	0.5	27.8	25.0	7.1	3.10		
$ST9_{deep}$	03/08/10 15:30	41° 12.434'	72° 58.669'	11	10	28	22.9	3.4	7.01		
$ST113E_{surf}$	05/08/10 10:25	41° 08.653'	72° 35.206'	22	0.5	28.2	24.5	7.2	1.25		
$ST113E_{deep}$	05/08/10 10:25	41° 08.653'	72° 35.206'	22	21	29.3	21.6	6.4	2.32		
$ST102_{surf}$	05/08/10 11:15	41° 10.139'	72° 27.721'	33	0.5	27.9	24.4	7.2	1.00	0.04	74
$ST102_{deep}$	05/08/10 11:15	41° 10.139'	72° 27.721'	33	31	29.8	22.0	6.7	1.51	0.02	323
$ST1_{surf}$	05/08/10 12:15	41° 14.948'	72° 19.928'	8	0.5	27.5	22.2	6.9	2.99		
$ST1_{deep}$	05/08/10 12:15	41° 14.948'	72° 19.928'	8	7	29.2	21.9	6.8	4.49		
$ST2_{surf}$	05/08/10 12:40	41° 13.092'	72° 19.920'	42	0.5	29	25.7	7.3	1.27		

ST2$_{deep}$	05/08/10 12:40	41° 13.092'	72° 19.920'	42	40	30.4	20.4	6.8	2.28		
ST3$_{surf}$	05/08/10 12:10	41° 11.556'	72° 19.919'	45	0.5	27.9	24.3	7.2	1.23	0.05	627
ST3$_{deep}$	05/08/10 12:10	41° 11.556'	72° 19.919'	45	42	30.3	20.4	6.7	1.30	0.05	9
ST4$_{surf}$	05/08/10 13:35	41° 09.547'	72° 19.922'	25	0.5	28	25.4	6.9	1.05		
ST4$_{deep}$	05/08/10 13:35	41° 09.547'	72° 19.922'	25	23	29.9	22.5	6.5	2.54		
ST10$_{surf}$	10/08/10 08:20	40° 56.326'	73° 11.609'	15	0.5	27.3	23.1	5.9	1.05		
ST10$_{deep}$	10/08/10 08:20	40° 56.326'	73° 11.609'	15	14	28	21.9	3.2	5.48		
ST120E$_{surf}$	10/08/10 09:10	41° 01.960'	73° 13.500'	30	0.5	27.5	23.3	7.0	1.65	0.41	122
ST120E$_{deep}$	10/08/10 09:10	41° 01.960'	73° 13.500'	30	29	28.4	21.3	4.0	6.05	0.32	117
ST120W$_{surf}$	10/08/10 10:15	40° 59.699'	73° 25.201'	49	0.5	27.5	22.9	6.0	2.15	0.52	168
ST120W$_{deep}$	01/01/04 10:15	40° 59.699'	73° 25.201'	49	48	28.2	21.4	3.5	5.94	0.40	87
ST11$_{surf}$	10/08/10 11:15	40° 55.777'	73° 34.280'	16	0.5	27.1	23.5	7.0	2.24		
ST11$_{deep}$	10/08/10 11:15	40° 55.777'	73° 34.280'	16	15	27.4	21.4	2.2	3.26		
ST12$_{surf}$	10/08/10 11:40	40° 56.510'	73° 34.618'	18	0.5	27.1	24.2	6.8	2.53		
ST12$_{deep}$	10/08/10 11:40	40° 56.510'	73° 34.618'	18	17	27.7	21.4	2.6	4.97		
ST14$_{surf}$	10/08/10 12:15	40° 58.898'	73° 36.487'	16	0.5	27.3	24.2	7.5	2.08		
ST14$_{deep}$	10/08/10 12:15	40° 58.898'	73° 36.487'	16	15	27.8	22.0	3.3	5.23		
ST15$_{surf}$	10/08/10 12:45	40° 58.303'	73° 35.739'	19	0.5	27.2	24.1	7.2	1.80		
ST15$_{deep}$	10/08/10 12:45	40° 58.303'	73° 35.739'	19	18	27.8	21.5	3.1	5.26		
ST13$_{surf}$	10/08/10 13:50	40° 57.439'	73° 35.365'	21	0.5	27.1	24.5	7.3	2.31	0.59	149
ST13$_{deep}$	10/08/10 13:50	40° 57.439'	73° 35.365'	21	20	27.8	21.6	3.1	5.03	0.44	91
ST17$_{surf}$	12/08/10 10:30	40° 55.109'	73° 40.243'	16	0.5	27.2	23.0	6.2	2.75		
ST17$_{deep}$	12/08/10 10:30	40° 55.109'	73° 40.243'	16	15	27.5	21.2	2.0	7.08		
ST18$_{surf}$	12/08/10 10:40	40° 48.020'	73° 47.356'	34	0.5	26.3	22.7	2.8	5.49		
ST18$_{deep}$	12/08/10 10:40	40° 48.020'	73° 47.356'	34	33	26.6	22.5	2.8	6.43		
ST16$_{surf}$	12/08/10 12:25	40° 52.463'	73° 44.969'	20	0.5	27.2	22.6	4.2	3.50	0.66	122
ST16$_{deep}$	12/08/10 12:25	40° 52.463'	73° 44.969'	20	21	27.5	21.6	2.6	13.51	0.61	98

Supplemental Data - Table S2.

SPRING 2009	^{224}Ra dpm·100L^{-1}	^{223}Ra dpm·100L^{-1}	^{226}Ra dpm·100L^{-1}	^{228}Ra dpm·100L^{-1}
$ST1_{surf}$	8.4 ± 0.6	0.57 ±0.21		
$ST1_{deep}$	7.3 ± 1.0	0.49 ±0.17		
$ST2_{surf}$	5.9 ± 0.4	1.15 ±0.28	5.7± 0.7	35± 4
$ST2_{deep}$	5.3 ± 0.4	0.50 ±0.17	5.6± 0.6	27± 5
$ST3_{surf}$	5.3 ± 0.4	0.41 ±0.13	5.9± 1.1	32± 4
$ST3_{deep}$	5.5 ± 0.4	0.68 ±0.16	6.7± 1.1	24± 4
$ST4_{surf}$	6.4 ± 0.4	0.54 ±0.16		
$ST4_{deep}$	4.5 ± 0.6	0.53 ±0.12		
$ST101_{surf}$	3.7 ± 0.4	0.80 ±0.16	5.8± 0.5	19± 3
$ST101_{deep}$	3.6 ± 0.2	0.35 ±0.11	5.3± 0.5	29± 3
$ST102_{surf}$	5.3 ± 0.4	0.43 ±0.11	6.2± 0.5	22± 4
$ST102_{deep}$	5.6 ± 0.3	0.59 ±0.12	6.3± 0.5	28± 4
$ST5_{surf}$	5.7 ± 0.3	0.51 ±0.13	8.5± 1.3	63± 5
$ST5_{deep}$	4.4 ± 0.6	0.29 ±0.08	8.9± 1.2	59± 5
$ST6_{surf}$	2.4 ± 0.2	0.20 ±0.08		
$ST6_{deep}$	5.1 ± 0.2	0.25 ±0.08		
$ST117_{surf}$	4.7 ± 0.2	0.40 ±0.09	10.8± 0.6	54± 5
$ST117_{deep}$	4.8 ± 0.2	0.43 ±0.08	11.4± 0.6	35± 5
$ST7_{surf}$	5.0 ± 0.4	0.63 ±0.18	10.1± 1.4	64± 6
$ST7_{5m}$	3.1 ± 0.4	0.37 ±0.11		
$ST7_{15m}$	4.4 ± 0.3	0.32 ±0.11		
$ST7_{deep}$	4.0 ± 0.3	0.28 ±0.09	8.9± 1.3	57± 5
$ST8_{surf}$	5.5 ± 0.4	0.56 ±0.13	9.1± 1.2	52± 5
$ST8_{deep}$	4.8 ± 0.6	0.77 ±0.20	9.7± 1.1	60± 4
$ST113_{surf}$	3.7 ± 0.4	0.25 ±0.09	10.7± 0.6	61± 5
$ST113_{deep}$	6.3 ± 0.3	0.37 ±0.11	10.6± 0.5	57± 4
$ST9_{surf}$	6.2 ± 0.3	0.70 ±0.15		
$ST9_{deep}$	10.5 ± 0.5	0.80 ±0.16		
$ST11_{surf}$	4.6 ± 0.3	0.79 ±0.19		
$ST11_{deep}$	7.0 ± 0.9	0.71 ±0.14		
$ST13_{surf}$	3.3 ± 0.4	0.45 ±0.11	8.4± 1.2	38± 6
$ST13_{deep}$	7.6 ± 0.3	0.56 ±0.16	9.5± 1.3	61± 5
$ST15_{surf}$	4.1 ± 0.2	0.47 ±0.10		
$ST15_{deep}$	6.5 ± 0.3	0.52 ±0.11		
$ST12_{surf}$	3.7 ± 0.3	0.60 ±0.17		
$ST12_{deep}$	7.7 ± 1.0	0.84 ±0.18		
$ST14_{surf}$	3.7 ± 0.4	0.44 ±0.13		
$ST14_{deep}$	7.4 ± 0.4	0.40 ±0.14		

$ST10_{surf}$	7.2 ± 0.4	0.56 ±0.14		
$ST10_{deep}$	6.8 ± 0.4	0.53 ±0.12		
$ST120W_{surf}$	4.3 ± 0.6	0.53 ±0.12	10.0± 1.5	66± 7
$ST120W_{deep}$	5.4 ± 0.4	0.25 ±0.11	12.0± 1.5	77± 8
$ST120E_{surf}$	4.0 ± 0.4	0.45 ±0.12	12.6± 1.5	86± 7
$ST120E_{deep}$	4.9 ± 0.3	0.42 ±0.13	11.1± 1.4	76± 6
$ST16_{surf}$	6.3 ± 0.4	0.54 ±0.13	8.5± 1.2	65± 5
$ST16_{deep}$	9.1 ± 0.4	0.83 ±0.16	7.5± 1.3	63± 5

Supplemental Data - Table S2 (continuation).

SUMMER 2009	^{224}Ra dpm·100L^{-1}	^{223}Ra dpm·100L^{-1}	^{226}Ra dpm·100L^{-1}	^{228}Ra dpm·100L^{-1}
$ST1_{surf}$	8.8 ± 0.5	1.3 ±0.3	9.4± 0.8	51± 5
$ST1_{deep}$	6.0 ± 0.3	0.9 ±0.2	10.5± 0.9	28± 6
$ST3_{surf}$	5.7 ± 0.4	0.9 ±0.2	8.2± 1.0	44± 6
$ST3_{deep}$	7.7 ± 0.5	0.8 ±0.2	9.9± 0.8	52± 5
$ST102_{surf}$	6.2 ± 0.5	0.8 ±0.2	10.0± 0.5	52± 3
$ST102_{deep}$	7.5 ± 0.5	0.7 ±0.2	8.9± 0.5	40± 3
$ST113E_{surf}$	8.6 ± 0.5	1.2 ±0.3	9.2± 0.5	54± 4
$ST113E_{deep}$	7.8 ± 0.5	0.8 ±0.2	9.2± 0.6	42± 4
$ST113W_{surf}$	4.2 ± 0.3	0.8 ±0.2	8.3± 0.6	31± 4
$ST113W_{deep}$	17.1 ± 0.8	1.5 ±0.3	8.1± 0.5	41± 3
$ST7_{surf}$	4.1 ± 0.4	1.1 ±0.3	9.7± 1.0	66± 7
$ST7_{deep}$	13.0 ± 0.8	1.1 ±0.3	11.4± 1.0	64± 8
$ST117_{surf}$	11.1 ± 0.7	1.0 ±0.3	11.5± 0.7	74± 5
$ST117_{deep}$	12.7 ± 0.8	1.3 ±0.3	10.0± 0.6	63± 5
$ST120E_{surf}$	8.5 ± 0.6	1.4 ±0.3	13.8± 1.1	97± 5
$ST120E_{deep}$	13.0 ± 0.7	0.9 ±0.2	12.1± 1.1	99± 8
$ST120W_{surf}$	9.9 ± 0.5	1.2 ±0.3	7.9± 1.0	65± 6
$ST120W_{deep}$	12.2 ± 0.6	1.2 ±0.2	15.2± 1.1	101± 8
$ST13_{surf}$	11.4 ± 0.7	1.7 ±0.4	13.2± 1.1	101± 8
$ST13_{deep}$	16.2 ± 0.9	1.7 ±0.4	15.0± 0.8	116± 6
$ST16_{surf}$	20.8 ± 1.1	1.6 ±0.4	16.7± 1.1	123± 8
$ST16_{deep}$	20.6 ± 1.2	1.5 ±0.4	13.9± 1.1	99± 7

Supplemental Data - Table S2 (continuation).

SUMMER 2010	^{224}Ra dpm·100L^{-1}	^{223}Ra dpm·100L^{-1}	^{226}Ra dpm·100L^{-1}	^{228}Ra dpm·100L^{-1}

$ST1_{surf}$	13.3 ± 0.8	1.33 ±0.17		
$ST1_{deep}$	13.9 ± 0.8	0.77 ±0.11		
$ST2_{surf}$	4.5 ± 0.3	0.53 ±0.07		
$ST2_{deep}$	6.8 ± 0.6	0.71 ±0.12		
$ST3_{surf}$	3.65 0.29	0.58 ±0.08	10.1± 1.6	77± 5
$ST3_{deep}$	6.83 0.45	0.89 ±0.13	11.4± 1.5	53± 5
$ST4_{surf}$	7.13 0.32	0.54 ±0.54		
$ST4_{deep}$	6.80 0.47	0.90 ±0.90		
$ST102_{surf}$	4.0 ± 0.2	0.86 ±0.11		
$ST102_{deep}$	7.7 ± 0.4	0.97 ±0.15		
$ST113E_{surf}$	4.2 ± 0.3	0.76 ±0.10		
$ST113E_{deep}$	7.3 ± 0.6	0.75 ±0.13		
$ST113W_{surf}$	3.8 ± 0.2	0.95 ±0.13		
$ST113W_{deep}$	17.8 ± 1.1	1.29 ±0.17		
$ST5_{surf}$	5.4 ± 0.4	1.52 ±0.18		
$ST5_{deep}$	16.1 ± 0.9	1.51 ±0.21		
$ST6_{surf}$	4.0 ± 0.3	0.76 ±0.10		
$ST6_{deep}$	12.6 ± 1.0	1.29 ±0.18		
$ST7_{surf}$	2.8 ± 0.2	0.72 ±0.12	12.1± 1.3	72± 4
$ST7_{deep}$	12.2 ± 0.9	0.98 ±0.14	12.7± 1.5	73± 5
$ST8_{surf}$	5.2 ± 0.4	0.82 ±0.13		
$ST8_{deep}$	15.4 ± 1.0	1.39 ±0.17		
$ST9_{surf}$	20.4 ± 1.9	1.70 ±0.21		
$ST9_{deep}$	27.6 ± 2.6	1.91 ±0.23		
$ST117_{surf}$	10.8 ± 0.5	1.15 ±0.16		
$ST117_{deep}$	16.4 ± 1.0	0.91 ±0.11		
$ST10_{surf}$	11.9 ± 0.8	1.36 ±0.17		
$ST10_{deep}$	28.0 ± 1.7	2.79 ±0.40		
$ST120E_{surf}$	5.3 ± 0.4	0.71 ±0.11	9.9± 1.5	71± 6
$ST120E_{deep}$	12.5 ± 0.8	1.22 ±0.16	13.0± 1.4	86± 6
$ST120W_{surf}$	9.7 ± 0.6	1.01 ±0.15	10.8± 1.5	70± 6
$ST120W_{deep}$	13.8 ± 0.8	1.44 ±0.18	14.7± 1.9	91± 7
$ST11_{surf}$	12.6 ± 0.8	1.45 ±0.18		
$ST11_{deep}$	25.5 ± 1.5	2.24 ±0.24		
$ST12_{surf}$	10.6 ± 0.7	0.89 ±0.89		
$ST12_{deep}$	20.8 ± 1.4	1.44 ±1.44		
$ST13_{surf}$	6.0 ± 0.4	1.13 ±0.15	7.5± 1.4	53± 5
$ST13_{deep}$	17.1 ± 0.8	1.68 ±0.19	13.8± 1.7	87± 7
$ST14_{surf}$	11.5 ± 0.6	0.89 ±0.16		
$ST14_{deep}$	14.2 ± 0.8	1.60 ±0.20		
$ST15_{surf}$	5.9 ± 0.5	1.37 ±0.20		
$ST15_{deep}$	15.4 ± 1.3	1.93 ±0.21		
$ST17_{surf}$	14.9 ± 1.0	1.97 ±0.22		

$ST17_{deep}$	21.3 ± 1.3	1.57 ±0.19		
$ST18_{surf}$	23.6 ± 1.2	1.93 ±0.21		
$ST18_{deep}$	24.1 ± 1.2	2.04 ±0.21		
$ST16_{surf}$	19.0 ± 1.2	1.40 ±0.14	15.0± 1.8	109± 7
$ST16_{deep}$	17.4 ± 1.0	2.11 ±0.23	14.9± 1.5	119± 6

SD - Table 3

ST8			
Depth in core (cm)	Water content (%)	Sediment Organic Matter (%)	Mn (mmol·g^{-1})
0.5	77.4	6.0	27.1
1.0	68.4	6.1	8.5
1.5	68.3	6.3	10.1
2.0	66.5	6.1	9.1
2.5	65.7	6.1	7.9
3.0	64.6	5.6	7.5
4.0	63.6	5.7	6.5
5.0	64.0	6.0	5.9
6.0	65.1	5.9	5.4
ST16			
Depth in core (cm)	Water content (%)	Sediment Organic Matter (%)	Mn (mmol·g^{-1})
0.5	83.4	8.3	10.3
1.0	68.6	6.8	7.4
1.5	65.8	6.4	8.2
2.0	66.5	7.1	7.9
2.5	66.4	6.9	8.8
3.0	66.5	7.9	8.2
4.0	64.6	7.8	8.2
5.0	62.7	7.6	9.8
6.0	62.3	7.7	10.5

SD - Table 4

ST 8 (2010)

Depth in core (cm)	^{226}Ra (dpm·g^{-1})	^{228}Ra (dpm·g^{-1})	^{228}Th (dpm·g^{-1})
0-2.0	1.35 ± 0.03	1.98 ± 0.10	2.13 ± 0.06
2.0-4.0	1.46 ± 0.04	1.80 ± 0.12	2.18 ± 0.07
4.0-5.0	1.37 ± 0.03	1.90 ± 0.09	2.04 ± 0.05
5.0-7.0	1.39 ± 0.04	1.91 ± 0.11	1.89 ± 0.06
7.0-9.0	1.24 ± 0.04	2.00 ± 0.10	1.81 ± O.06
9.0-11.0	1.17 ± 0.04	2.32 ± 0.11	1.80 ± 0.06
11.0-13.0	1.35 ± 0.04	1.97 ± 0.11	1.83 ± 0.06
15.0-17.0	1.32 ± 0.04	2.20 ± 0.11	1.97 ± 0.07

ST 13 (2009)

Depth in core (cm)	^{226}Ra (dpm·g^{-1})	^{228}Ra (dpm·g^{-1})	^{228}Th (dpm·g^{-1})
0-2.0	1.24 ± 0.03	1.64 ± 0.07	n.m.
2.0-4.0	1.12 ± 0.02	1.54 ± 0.06	n.m.
4.0-6.0	1.22 ± 0.02	1.88 ± 0.06	n.m.
6.0-8.0	1.16 ± 0.02	1.49 ± 0.06	n.m.
8.0-10.0	1.27 ± 0.03	1.70 ± 0.08	n.m.
10.0-12.0	1.40 ± 0.02	1.70 ± 0.05	n.m.
12.0-14.0	1.27 ± 0.03	1.18 ± 0.07	n.m.
14.0-16.0	1.43 ± 0.02	1.85 ± 0.05	n.m.

ST 16 (2010)

Depth in core (cm)	^{226}Ra (dpm·g^{-1})	^{228}Ra (dpm·g^{-1})	^{228}Th (dpm·g^{-1})
0-1.5	1.09 ± 0.02	1.83 ± 0.02	2.13 ± 0.01
1.5-3.0	0.94 ± 0.04	1.65 ± 0.04	1.73 ± 0.02
3.0-5.0	1.05 ± 0.03	1.81 ± 0.03	2.18 ± 0.01
5.0-7.0	1.19 ± 0.03	2.00 ± 0.03	2.25 ± 0.01
7.0-9.0	1.08 ± 0.03	2.12 ± 0.02	2.11 ± 0.02
9.0-11.0	1.19 ± 0.02	2.10 ± 0.02	2.14 ± 0.01
11.5-13.5	1.13 ± 0.02	2.08 ± 0.02	2.15 ± 0.01
15.0-17.0	1.08 ± 0.03	2.24 ± 0.02	2.40 ± 0.01

ST 120E (2009)

Depth in core (cm)	^{226}Ra (dpm·g^{-1})	^{228}Ra (dpm·g^{-1})	^{228}Th (dpm·g^{-1})
0-2.0	1.40 ± 0.03	2.50 ± 0.09	n.m.
2.0-4.0	1.34 ± 0.03	2.40 ± 0.08	n.m.
4.0-6.0	1.33 ± 0.02	1.91 ± 0.07	n.m.

6.0-8.0	1.29 ± 0.03	1.99 ± 0.08	n.m.
8.0-10.0	1.36 ± 0.03	1.70 ± 0.08	n.m.
10.0-12.0	1.33 ± 0.02	2.00 ± 0.05	n.m.
12.0-14.0	1.38 ± 0.03	2.40 ± 0.08	n.m.

ST MW (2009)

Depth in core (cm)	^{226}Ra (dpm·g^{-1})	^{228}Ra (dpm·g^{-1})	^{228}Th (dpm·g^{-1})
0-1.0	0.30 ± 0.01	0.40 ± 0.02	n.m.
1.0-3.0	0.33 ± 0.01	0.34 ± 0.02	n.m.
3.0-5.0	0.36 ± 0.01	0.39 ± 0.02	n.m.
5.0-7.0	0.42 ± 0.01	0.46 ± 0.02	n.m.
7.0-9.0	0.53 ± 0.01	0.60 ± 0.02	n.m.
9.0-11.0	0.40 ± 0.01	0.48 ± 0.02	n.m.
11.0-13.0	0.37 ± 0.01	0.39 ± 0.02	n.m.
13.0-15.0	0.35 ± 0.01	0.38 ± 0.02	n.m.

SD - Table 5

ST 13 (2009)

Depth in core (cm)	^{224}Ra (dpm·L^{-1})	^{223}Ra (dpm·L^{-1})
0-2.0	14.4 ± 0.7	0.44 ± 0.16
2.0-4.0	14.7 ± 0.9	0.90 ± 0.28
4.0-6.0	12.7 ± 0.9	1.28 ± 0.37
7.0-9.0	14.6 ± 1.1	1.21 ± 0.37
10.0-12.0	17.2 ± 1.0	0.96 ± 0.26
12.0-14.0	13.2 ± 1.0	0.31 ± 0.19
14.0-16.0	17.9 ± 1.1	0.67 ± 0.24
16.0-19.0	17.6 ± 0.7	1.22 ± 0.26

ST 120E (2010)

Depth in core (cm)	^{224}Ra (dpm·L^{-1})	^{223}Ra (dpm·L^{-1})
0-2.0	16.0 ± 0.7	0.62 ± 0.19
2.0-4.0	22.4 ± 1.3	1.31 ± 0.40
4.0-6.0	16.4 ± 0.9	0.91 ± 0.26
8.0-10.0	15.3 ± 0.8	0.99 ± 0.26
10.0-12.0	14.0 ± 0.9	0.52 ± 0.22
12.0-14.0	19.3 ± 1.1	1.20 ± 0.34
14.0-16.0	17.2 ± 1.0	1.10 ± 0.33